

Quantifying Epistemic Predictive Uncertainty in Conformal Prediction

Siu Lun Chau¹, Soroush H. Zargarbashi², Yusuf Sale^{3,4}, and Michele Caprio^{5, 6}

¹Epistemic Intelligence & Computation Lab, College of Computing & Data Science, Nanyang Technological University, Singapore

²CISPA Helmholtz Center for Information Security, Germany

³Munich Center for Machine Learning; Institute of Informatics, LMU Munich, Germany

⁴Munich Center for Machine Learning, Germany

⁵Manchester Centre for AI Fundamentals, Manchester, United Kingdom

⁶Department of Computer Science, The University of Manchester, United Kingdom

February 3, 2026

Abstract

We study the problem of quantifying epistemic predictive uncertainty (EPU)—that is, uncertainty faced at prediction time due to the existence of multiple plausible predictive models—within the framework of conformal prediction (CP). To expose the implicit model multiplicity underlying CP, we build on recent results showing that, under a mild assumption, any full CP procedure induces a set of closed and convex predictive distributions, commonly referred to as a credal set. Importantly, the conformal prediction region (CPR) coincides exactly with the set of labels to which all distributions in the induced credal set assign probability at least $1 - \alpha$. As our first contribution, we prove that this characterisation also holds in split CP. Building on this connection, we then propose a computationally efficient and analytically tractable uncertainty measure, based on *Maximum Mean Imprecision*, to quantify the EPU by measuring the degree of conflicting information within the induced credal set. Experiments on active learning and selective classification demonstrate that the quantified EPU provides substantially more informative and fine-grained uncertainty assessments than reliance on CPR size alone. More broadly, this work highlights the potential of CP serving as a principled basis for decision-making under epistemic uncertainty.

Keywords: Conformal prediction, imprecise probabilities, predictive uncertainty quantification

1 Introduction

Conformal prediction (CP) (Shafer & Vovk, 2008) is a set-based uncertainty quantification framework that guarantees finite-sample coverage under the assumption that the data generating process is exchangeable. Owing to its conceptual simplicity and seamless integration into existing machine learning (ML) pipelines, CP has seen broad adoption in both theoretical and applied work (Balasubramanian et al., 2014).

In this work, *we study the problem of quantifying the epistemic predictive uncertainty (EPU) for conformal prediction*. Like the broader distinction between general “aleatoric” (inherent stochasticity) and “epistemic”(reducible knowledge-level) uncertainty, EPU does not admit one precise mathematical definition (Hüllermeier & Waegeman, 2021). Instead, it is typically characterised

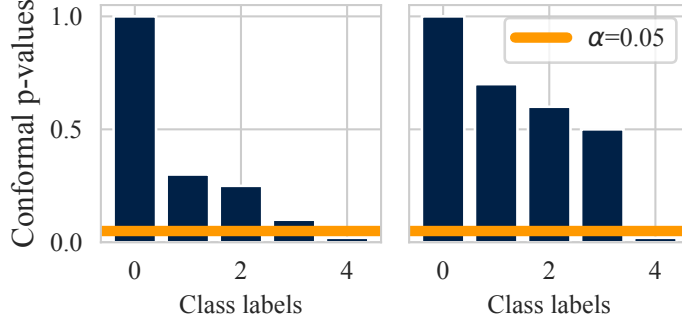


Figure 1: Although the two instances share the same prediction set, the left instance is evidently more certain, as reflected by uniformly smaller conformal p-values for labels (1, 2, 3). How can this intuition be formalised?

conceptually as “*the difficulty of making predictions about outcome Y given an observation $X = x$ due to model uncertainty, i.e., when multiple plausible predictive models exist.*” Crucially, EPU pertains to uncertainty of performing a prediction, rather than uncertainty intrinsic to the predicted outcome. For instance, in Bayesian ML, model uncertainty is represented via a posterior distribution $P(\theta | D)$ over model parameters θ after observing dataset D . Through information-theoretic approaches, EPU is then quantified by measuring the average reduction in predictive entropy after conditioning on model parameter θ (Kendall & Gal, 2017). Beyond trustworthiness and interpretability, quantifying EPU enables a principled separation from aleatoric uncertainty, supporting and improving downstream decision-making tasks that rely on the numerical assessment of model predictive confidence, such as active learning (Settles, 2009), learning to reject (Cortes et al., 2016) and defer (Madras et al., 2018), and Bayesian optimisation (Shahriari et al., 2015).

In contrast to Bayesian ML (Gal et al., 2016), the problem of quantifying EPU within CP has received comparatively little attention. This may be because it appears to admit a seemingly natural proxy: the size of the conformal prediction region (CPR) (Karimi & Samavi, 2023), measured as the number of elements in the prediction set for classification and as the interval length for regression. However, the CPR size at a fixed level α characterises uncertainty about the predicted region itself, rather than the uncertainty encountered when producing that prediction. As such, it does not directly quantify EPU. This limitation is analogous to assessing epistemic predictive uncertainty in Bayesian models solely via a $(1 - \alpha)\%$ highest density region of the posterior predictive (Hyndman, 1996) (Figure 2a). While such regions may correlate with EPU in certain scenarios, they are not designed to capture uncertainty in the predictive mechanism as a whole. As a concrete example, Figure 1 shows two predictions that yield identical CPRs at $\alpha = 0.05$, yet exhibit markedly different “confidence profiles”: one is supported by a much more skewed conformal p-value distribution than the other, indicating different levels of difficulties encountered when constructing the prediction set. This observation motivates our central goal: to formalise such intuition within a rigorous mathematical framework and to characterise epistemic predictive uncertainty through the structure of these conformal p-value profiles.

Contributions. To achieve our goal, we build on recently established connections between conformal prediction and imprecise probabilities (IP) (Walley, 1991), a framework that generalises classical probability theory to model higher-order uncertainty through non-linear expectations (Troffaes & de Cooman, 2014) and sets of probability measures, known as credal sets (Levi, 1980). In particular,

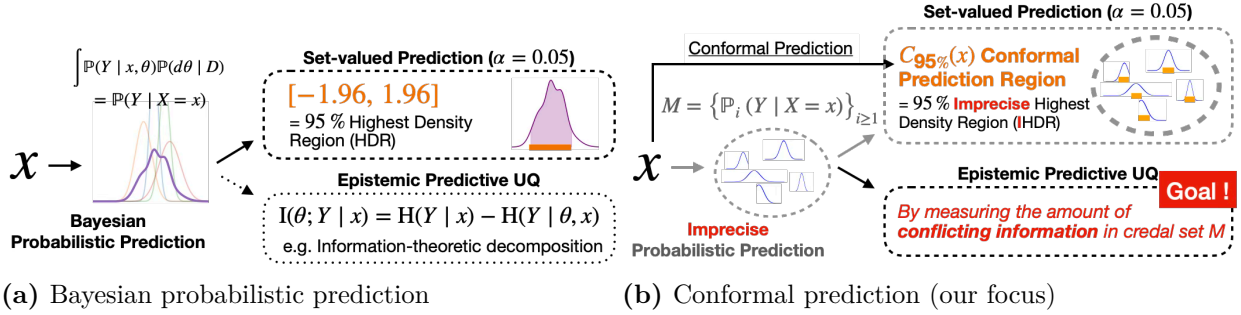


Figure 2: Instead of distribution of plausible models as in Bayesian prediction, conformal prediction implicitly yields a set of plausible models as shown by (Cella & Martin, 2022). How can we quantify the epistemic predictive uncertainty in this case?

Cella & Martin (2022) demonstrated that, under a mild technical assumption, any full (transductive) CP procedure induces a credal set of predictive distributions over the target variable Y . This result was subsequently strengthened by Caprio et al. (2025c); Caprio (2025b), who proved that CPRs coincide with imprecise highest density regions (Coolen, 1992), i.e., the generalisation of highest density regions to sets of probabilities associated with such predictive credal sets.

Taken together, these results imply that *every full CP procedure implicitly induces a predictive credal set* (Figure 2b). Building on this line of work, we further show that these guarantees, previously established only for full CP, also hold for split (inductive) CP (Papadopoulos et al., 2002), which is more commonly used in practice for computational efficiency. This extension provides the mathematical foundation for our approach to quantifying EPU in CP by **measuring the degree of “conflicting information” encoded in the implicit predictive credal set**. This perspective aligns with recent approaches to quantifying EPU for imprecise probabilistic predictors, i.e. models that return credal sets as predictions (Wang et al., 2024, 2025a,b; Caprio et al., 2024a, 2025b). However, unlike these settings—where predictive credal sets are typically constructed as convex hulls of finitely many probabilistic predictors—the implicit predictive credal set in CP arises as a set of distributions dominated by a single imprecise probability measure (Dubois & Hüllermeier, 2007), as characterised by Martin (2025, Theorem 1.). This structural distinction motivates us to build on and adapt the recently introduced EPU quantification functional, the maximum mean imprecision (MMI) (Chau et al., 2025), to the conformal setting. We refer to our resulting methodology as **MMI-CP**.

Paper structure. The paper is structured as follows. Section 2 reviews CP and IP, followed by our main results and derivations of MMI-CP in Section 3. Section 4 discusses related work, Section 5 presents empirical results, and Section 6 concludes with discussions. All proofs and derivations can be found in Appendix C.

2 Preliminaries

Notations. Let \mathcal{X}, \mathcal{Y} denote input and output spaces, respectively, with $\mathcal{Y} = \{y^{(k)}\}_{k=1}^K$ for K -class classification and $\mathcal{Y} = \mathbb{R}$ for regression. Uppercase letters X, Y denote random variables on \mathcal{X}, \mathcal{Y} , and lowercase letters x, y their realisations. Let $D = \{(x_i, y_i)\}_{i=1}^n$ be exchangeable samples from our data-generating process. We denote $\mathcal{P}(\mathcal{Y})$ the space of all probability measures on our measurable output space $(\mathcal{Y}, \mathcal{F}_{\mathcal{Y}})$.

2.1 Split Conformal Prediction

We adopt the split CP framework (Papadopoulos et al., 2002) in this work. We assume access to dataset D_{cal} of size n_{cal} , along with a predictive model $\hat{f} : \mathcal{X} \rightarrow \Delta_{K-1}$ (the $K-1$ dimensional probability simplex) for K -class classification and $\hat{f} : \mathcal{X} \rightarrow \mathbb{R}$ for regression. Let $s : \mathcal{X} \times \mathcal{Y} \rightarrow \mathbb{R}$ denote a *non-conformity score* function that quantifies how atypical a candidate example is with respect to the predictive model \hat{f} and the calibration dataset D_{cal} . Applying s to the calibration set yields the calibration scores

$$S_{\text{cal}} = \{s(x_i, y_i) : (x_i, y_i) \in D_{\text{cal}}\}.$$

For simplicity, we write $s_i = s(x_i, y_i)$ below.

Given a user-specified error tolerance $\alpha \in (0, 1)$ and a test input x , the conformal prediction region (CPR) is given by

$$C_\alpha(x) := \{y \in \mathcal{Y} : s(x, y) \leq \hat{q}_{1-\alpha}\},$$

where $\hat{q}_{1-\alpha}$ denotes the empirical $(1 - \alpha)$ -quantile of the calibration scores S_{cal} , that is, $\hat{q}_{1-\alpha} = s_{\sigma(k)}$ where $k = \lceil (1 - \alpha)(n_{\text{cal}} + 1) \rceil$ and σ denoting a permutation that orders the calibration scores in nondecreasing order. Under the exchangeability assumption in the observations, this construction ensures that, for an unseen data point (X_{n+1}, Y_{n+1}) , the CPR satisfies

$$\mathbb{P}(Y_{n+1} \in C_\alpha(X_{n+1})) \geq 1 - \alpha.$$

In practice, calibration scores S_{cal} may contain ties, which can affect the coverage guarantee of CP. A standard remedy is to apply randomised tie-breaking, for example, by defining $\tilde{s}_i = s_i + \epsilon u_i$ where $u_i \sim \text{U}[0, 1]$ and $\epsilon > 0$ arbitrarily small. For notational clarity, we assume such a tie-breaking mechanism throughout and write s_i in place of \tilde{s}_i .

Equivalently, the CPR can be expressed as $C_\alpha(x) := \{y \in \mathcal{Y} : \pi_x(y) > \alpha\}$, where

$$\pi_x(y) = \frac{1 + |i \in \{1, \dots, n_{\text{cal}}\} : s_i \geq s(x, y)|}{1 + n_{\text{cal}}}.$$

The function $\pi_x : \mathcal{Y} \rightarrow [0, 1]$ is referred to as the *conformal transducer* (Vovk & Bendtsen, 2018) and the value $\pi_x(y)$ is called the conformal p-value. It can be interpreted as the p-value associated with testing the null hypothesis $H_0 : D_{\text{cal}} \cup \{(x, y)\}$ is exchangeable. This characterisation, later in Section 3, allows us to connect CP to imprecise probabilities, which we introduce next.

2.2 Imprecise probabilities

Imprecise probabilities (IP) (Walley, 1991; Augustin et al., 2014) generalise classical probability (Kolmogorov, 1933) to model higher-order uncertainties through non-linear expectations (Troffaes & de Cooman, 2014) and **sets of probability measures**, typically assumed to be convex and closed, known as **credal sets** $\mathcal{M} \subseteq \mathcal{P}(\mathcal{Y})$. Credal sets are used to represent ambiguity, conflict of evidence (Destercke, 2010), and ignorance of a learning agent (Williamson, 2010).

Credal sets. Credal sets have recently received growing attention in ML as an uncertainty modelling framework. They enable a clear distinction between aleatoric uncertainty, associated with individual probability measures within the set, and epistemic uncertainty, which is captured by the set as a whole. Common constructions of a credal set \mathcal{M} include taking the convex hull of a collection of probabilistic predictors, such as those arising from deep ensembles (Wang et al., 2024)

or multi-objective optimisation procedures (Caprio et al., 2024a), as well as defining \mathcal{M} through sets of empirical distributions, as commonly encountered in multi-source learning settings (Singh et al., 2024, 2025b; Chau et al., 2024).

Capacities, upper probabilities, and cores. Beyond convex hull constructions, credal sets can also be generated via probability bounds, such as those induced by capacities and upper probabilities (Choquet, 1953).

Definition 2.1 (Capacities and Upper probabilities (Cerreia-Vioglio et al., 2016)). A set function $\bar{\mathbb{P}} : \mathcal{F}_{\mathcal{Y}} \rightarrow [0, 1]$ is a capacity if

1. $\bar{\mathbb{P}}(\emptyset) = 0, \bar{\mathbb{P}}(\mathcal{Y}) = 1$, and
2. $\bar{\mathbb{P}}(A) \leq \bar{\mathbb{P}}(B)$ for $A \subseteq B$ with $A, B \in \mathcal{F}_{\mathcal{Y}}$.

Furthermore, if there also exists a compact set $\mathcal{M} \subseteq \mathcal{P}(\mathcal{Y})$ where

$$\bar{\mathbb{P}}(A) = \sup_{\mathbb{P} \in \mathcal{M}} \mathbb{P}(A)$$

for all $A \in \mathcal{F}_{\mathcal{Y}}$, then $\bar{\mathbb{P}}$ is also an upper probability.

Capacity can be viewed as one of the simplest forms of uncertainty representation: a monotonic set function over events. However, in its full generality, it is often too flexible for practical use, which has motivated the study of capacities with additional structure, such as upper probabilities and standard probability measures.

An upper probability admits a dual representation, known as *lower probability*, defined as

$$\underline{\mathbb{P}}(A) = 1 - \bar{\mathbb{P}}(A^c)$$

for $A \in \mathcal{F}_{\mathcal{Y}}$. This duality admits an intuitive interpretation: while $\bar{\mathbb{P}}(A)$ encodes direct belief that an event A occurs, its conjugate $\underline{\mathbb{P}}$ encodes belief in A indirectly, by quantifying the degree of disbelief in its complement A^c . An upper probability can be constructed by taking the event-wise supremum over a finite collection of probability measures, i.e.,

$$\bar{\mathbb{P}}(A) = \sup_{\mathbb{P} \in \{\mathbb{P}_1, \dots, \mathbb{P}_M\}} \mathbb{P}(A),$$

for all $A \in \mathcal{F}_{\mathcal{Y}}$. Under this interpretation, model uncertainty is naturally represented by the set of probability measures set-wise dominated by these upper bounds. This is known as the *core* of $\bar{\mathbb{P}}$ and forms a credal set. We present the general definition of a core, defined via capacities,

Definition 2.2 (Core). The core of a capacity $\bar{\mathbb{P}}$ is given by

$$\mathcal{M}(\bar{\mathbb{P}}) := \{\mathbb{P} \in \mathcal{P}(\mathcal{Y}) : \mathbb{P}(A) \leq \bar{\mathbb{P}}(A) \text{ for all } A \in \mathcal{F}_{\mathcal{Y}}\}.$$

Quantifying EPU of credal predictors. The amount of conflicting probabilistic information of a predictive credal set provides a means of gauging the difficulty of predicting the true label Y for a new input x under model uncertainty (Hofman et al., 2024). Several uncertainty measures have been proposed in the literature. For example, one may consider the maximum difference in entropy between any distributions in the credal set \mathcal{M} , but it has been shown to be suboptimal (Sale et al., 2023) as they fail to satisfy desirable axioms of uncertainty quantification (Abellán et al., 2006). Another common approach generalises the classical Hartley measure (Hartley, 1928) to IP settings.

Such measures, however, often incur exponential computational complexity in the number of classes for classification and have not been defined for continuous state space (regression) settings.

In light of these limitations, Chau et al. (2025) recently proposed an alternative based on integral imprecise probability metrics, termed the *Maximum Mean Imprecision* (MMI). This approach enjoys empirical performance comparable to that of the Generalised Hartley measure, while admitting a linear-time computable upper bound, rendering it tractable for classification problems with a large number of classes.

Definition 2.3 (MMI). Let $\bar{\mathbb{P}}$ be an upper probability and \mathcal{H} be a set of test functions $h : \mathcal{Y} \rightarrow \mathbb{R}$. The Maximum Mean Imprecision is given by

$$\text{MMI}_{\mathcal{H}}(\bar{\mathbb{P}}) = \sup_{h \in \mathcal{H}} \left| \int h d\bar{\mathbb{P}} - \int h d\underline{\mathbb{P}} \right|,$$

where \int is the Choquet integral (Choquet, 1953).

Further technical details and background on MMI are provided in Appendix B. Building on the duality between upper and lower probabilities, the MMI measures the degree of conflicting information by the largest discrepancy, over a prescribed class of test functions, between optimistic and pessimistic expectations. A standard choice of test function class for classification is the set of indicator functions: $\mathcal{H}_{\text{TV}} = \{\mathbf{1}_A : A \in \mathcal{F}_{\mathcal{Y}}\}$, reducing the MMI in total-variation-like metric:

$$\text{MMI}_{\mathcal{H}_{\text{TV}}}(\bar{\mathbb{P}}) = \sup_{A \in \mathcal{F}_{\mathcal{Y}}} |\bar{\mathbb{P}}(A) - \underline{\mathbb{P}}(A)|.$$

In the next section, we show that, under a mild technical assumption, conformal transducers naturally induce a class of upper probabilities known as plausibility measures (De Cooman, 1997). The core of the resulting upper probability—representing an implicit form of model uncertainty—can be used to recover the CPR exactly. By adapting the MMI to this core, we obtain a principled quantification of EPU associated with any conformal procedure.

3 Quantifying Epistemic Predictive Uncertainty in Conformal Prediction

3.1 Split CP admits an implicit predictive credal set

Recall from Section 2.1 that the CPR can be expressed as $C_{\alpha}(x) = \{y \in \mathcal{Y} : \pi_x(y) > \alpha\}$ where $\pi_x(\cdot)$ is the conformal transducer. We now state our technical assumption, called *consonance* (Cella & Martin, 2022).

Definition 3.1 (Consonance). A conformal transducer $\pi_x(\cdot)$ is consonant if $\sup_{y \in \mathcal{Y}} \pi_x(y) = 1$.

This condition holds in general for regression, e.g., consider the absolute residual error score $s(x, y) = |\hat{f}(x) - y|$, then $s(x, \hat{f}(x)) = 0$ implies $\pi_x(\hat{f}(x)) = 1$. However, this condition may fail in classification. Nevertheless, this issue can be circumvented by a simple construction: by stretching the largest conformal p-value to 1 (Cella & Martin, 2022, Section 7). Specifically, sort the labels $y_{\sigma(1)}, y_{\sigma(2)}, \dots, y_{\sigma(K)}$ by their conformal p-values in descending order, allowing ties but resolving them in a consistent manner, and set

$$\pi_x(y) \leftarrow \begin{cases} 1, & \text{if } y = y_{\sigma(1)} \\ \pi_x(y), & \text{otherwise.} \end{cases} \quad (1)$$

The theoretical and empirical implications of the consonance assumption are discussed in Section 3.3. In brief, this modification does not affect non-empty prediction sets, retains the marginal coverage guarantee in general, and crucially, it provides a stronger reliability property, known as Type II validity (Cella & Martin, 2022). Next, we derive the implicit predictive credal set based on the consonant transducer π_x .

Proposition 3.2. *Let π_x be consonant, define $\bar{\mathbb{P}}_x$ by*

$$\bar{\mathbb{P}}_x(A) = \sup_{y \in A} \pi_x(y)$$

for all $A \in \mathcal{F}_Y$, with the convention $\bar{\mathbb{P}}_x(\emptyset) := 0$. Then $\bar{\mathbb{P}}_x$ is an upper probability.

Proposition 3.2 shows that a consonant transducer induces an upper probability measure $\bar{\mathbb{P}}_x$ by assigning each event the maximum conformal p-value it contains. In IP, an upper probability with this special maxitive structure is known as a *plausibility measure* (Friedman & Halpern, 1995). We now show that the core $\mathcal{M}(\bar{\mathbb{P}}_x)$ admits a natural interpretation as the implicit predictive credal set underlying the corresponding CP procedure. To make this connection precise, we first recall the notion of a highest density region in the context of IP, which is usually introduced through lower probabilities.

Definition 3.3 (Imprecise Highest Density Region (Coolen, 1992)). Given a lower probability $\underline{\mathbb{P}}$ and $\alpha \in [0, 1]$, the set $\text{IR}_\alpha \subseteq \mathcal{Y}$ is a $(1 - \alpha)$ -*Imprecise Highest Density Region* (IHDR) if

$$\underline{\mathbb{P}}(Y \in \text{IR}_\alpha) = 1 - \alpha$$

and the size $\int_{\text{IR}_\alpha} dy$ is minimum. If \mathcal{Y} is at most countable, replace $\int_{\text{IR}_\alpha} dy$ with $|\text{IR}_\alpha|$.

An immediate consequence of this definition is that

$$\mathbb{P}(Y \in \text{IR}_\alpha) \geq 1 - \alpha$$

for all $\mathbb{P} \in \mathcal{M}(\bar{\mathbb{P}})$. Now we can state our first result connecting CPR with IHDRs for split CP, similar to Caprio et al. (2025c, Proposition 5) for full CP.

Proposition 3.4. *Denote the $(1 - \alpha)$ -IHDR of $\bar{\mathbb{P}}_x$ as $\text{IR}_\alpha^{\mathcal{M}}$. Then, for any $\alpha \in [0, 1]$, we have*

$$\text{IR}_\alpha^{\mathcal{M}} = C_\alpha(x).$$

Proposition 3.4 illustrates that, under the consonance assumption, any split conformal prediction procedure (also) admits an implicit predictive credal set that represents its model uncertainty. To quantify this uncertainty, we adopt the general MMI framework (Definition 2.3) to characterise the amount of conflicting information in $\mathcal{M}(\bar{\mathbb{P}}_x)$ via the associated upper probability $\bar{\mathbb{P}}_x$.

3.2 Quantifying EPU with MMI-CP

While Chau et al. (2025) introduced MMI for general upper probabilities, the ones considered here are plausibility measures with a maxitive structure, $\bar{\mathbb{P}}_x(A) = \sup_{y \in A} \pi_x(y)$, which enables a substantial computational simplification: exact MMI can be computed efficiently, whereas in the general case it requires exponential time.

Proposition 3.5. *Let $\mathcal{H}_{TV} = \{\mathbf{1}_A : A \in \mathcal{F}_Y\}$. Then*

$$\text{MMI}_{\mathcal{H}_{TV}}(\bar{\mathbb{P}}_x) = \sup_{A \in \mathcal{F}_Y} |\bar{\mathbb{P}}_x(A) - \underline{\mathbb{P}}_x(A)| = \pi_{\sigma(2)},$$

where $\pi_{\sigma(2)}$ denotes the second largest conformal p-value.

In classification, computing $\text{MMI}_{\mathcal{H}_{\text{TV}}}(\overline{\mathbb{P}_x})$ takes only $\mathcal{O}(K)$ time, compared to $\mathcal{O}(2^K)$ for general upper probability. An analogous reduction holds for regression, yielding $\mathcal{O}(n_{\text{cal}})$ complexity due to sorting. Proposition 3.5 admits a simple intuition. Under consonance, all prediction instances share the same largest conformal p-value, equal to 1, which is therefore non-informative. What distinguishes confidence in predictions is the distribution, or portfolio, of the remaining p-values. For instance, in Figure 1, although both instances yield prediction sets of identical size, the left instance exhibits uniformly smaller p-values than the right, indicating stronger evidence as to what labels to include or not. From this perspective, the second-largest p-value $\pi_{\sigma(2)}$, the maximum among all remaining p-values, serves as one concise summary of overall confidence.

However, while $\pi_{\sigma(2)}$ upper bounds the nontrivial p-values, it is also natural to consider measures that account for the entire p-value portfolio. This motivates us to propose a new characterisation of MMI for plausibility measures and CP, using the conformal transducer π_x as the test function.

Proposition 3.6. *Let π_x be consonant and $\overline{\mathbb{P}_x}$ the induced plausibility measure. Then,*

$$\text{MMI}_{\{\pi_x\}}(\overline{\mathbb{P}_x}) = \int_0^1 \sup_{y \notin C_\alpha(x)} \pi_x(y) d\alpha \quad (2)$$

$$= \int_0^1 (1 + n_{\text{cal}})^{-1} (1 + |B_\alpha|) d\alpha, \quad (3)$$

where $B_\alpha = \{S_i \in S_{\text{cal}} : S_i \geq \inf_{y \notin C_\alpha(x)} s(x, y)\}$.

Essentially, $\text{MMI}_{\{\pi_x\}}$ aggregates, across all confidence levels, the largest conformal p-values among labels excluded from the CPR. This perspective highlights that, as one would expect in split CP, the EPU quantified is intrinsically shaped by both the calibration set and the chosen nonconformity score. Next, we show that these quantification functions admit closed-form analytical expressions, leading to efficient and practically implementable solutions.

3.2.1 EPU in Conformal Classification

In conformal classification, $\text{MMI}_{\{\pi_x\}}$ can be expressed as:

Proposition 3.7. *For K -class classification,*

$$\text{MMI}_{\{\pi_x\}}(\overline{\mathbb{P}_x}) = \sum_{k=2}^{K+1} (\pi_{\sigma(k-1)} - \pi_{\sigma(k)}) \cdot \pi_{\sigma(k)},$$

where $\pi_{\sigma(1)} \geq \pi_{\sigma(2)} \cdots \geq \pi_{\sigma(K)}$ are conformal p-values arranged in descending order, and $\pi_{(K+1)} := 0$.

Interestingly, instead of simply summing up the p-values, $\text{MMI}_{\{\pi_x\}}$ explicitly accounts for the discrete ‘‘gradients’’ of the p-value profile, namely the consecutive differences $\pi_{\sigma(k-1)} - \pi_{\sigma(k)}$. This aligns well with intuition: a large gap between consecutive sorted p-values indicates a highly skewed p-value distribution, in which a few classes receive substantially stronger support than the others. In such situations, the conformal procedure can more easily discriminate between plausible and implausible labels, making the construction of the conformal prediction set more decisive.

3.2.2 EPU in Conformal Regression

For conformal regression, $\text{MMI}_{\{\pi_x\}}$ exhibits a different phenomenon than in classification.

Proposition 3.8. *In conformal regression, for score functions satisfying $\inf_{y \notin C_\alpha(x)} s(x, y) = \hat{q}_{1-\alpha}$,*

$$\text{MMI}_{\{\pi_x\}}(\overline{\mathbb{P}_x}) = 1 + \int_0^1 \frac{1 - \lceil (n_{\text{cal}} + 1)(1 - \alpha) \rceil}{n_{\text{cal}} + 1} d\alpha.$$

Proposition 3.8 implies that for scores satisfying conditions $\inf_{y \notin C_\alpha(x)} s(x, y) = \hat{q}_{1-\alpha}$, the quantified EPU is constant across any prediction instances x . This might look counterintuitive at first, especially when the condition is met by many standard regression scores $s(x, \cdot)$ that are continuous and monotonic in y and can take values in \mathbb{R}_+ , such as

- **absolute residual:** $s_1(x, y) = |y - \hat{f}(x)|$,
- **weighted residual:** $s_2(x, y) = |y - \hat{f}(x)|/w(x)$, and
- **quantile regression score:** $s_3(x, y) = \max\{\hat{f}_\ell(x) - y, y - \hat{f}_u(x)\}$,

where $w(x)$ denotes certain weights and \hat{f}_ℓ, \hat{f}_u denotes certain quantile regressors. Nonetheless, this observation is consistent with existing findings that conformal regression is generally poor at distinguishing test instances based on the sizes of their prediction intervals (Boström & Johansson, 2020). In particular, when using the absolute residual score s_1 , the conformal prediction region takes the form

$$[\hat{f}(x) \pm \hat{q}_{1-\alpha}],$$

whose length $2\hat{q}_{1-\alpha}$ is uniform across all test instances. Even when employing score functions that yield adaptive intervals, such adaptivity arises from information encoded in the predictive model \hat{f} or in the estimated quantile functions \hat{f}_ℓ and \hat{f}_u , rather than from the conformal procedure. This is apparent when we examine the interval lengths $2\hat{q}_{1-\alpha}w(x)$ and $2\hat{q}_{1-\alpha} + \hat{f}_u(x) - \hat{f}_\ell(x)$, obtaining from using scores s_2 and s_3 respectively. Since crucially, in all these cases, the conformal component—namely, the degree to which a test prediction deviates from the calibration set—remains unchanged across instances, as evidenced by the common appearance of the calibration quantile $\hat{q}_{1-\alpha}$ in all interval constructions. Consequently, although the resulting prediction intervals may vary in length, such variation does not reflect differences in epistemic predictive uncertainty induced by the conformal procedure itself.

3.2.3 Why the difference in Classification v.s. Regerssion?

Propositions 3.7 and 3.8 reveal a fundamental difference between EPU in classification and regression. This contrast stems from how the nonconformity score behaves as a function of the output variable y , which in turn determines what information the conformal procedure can extract from the calibration data.

In classification, the nonconformity score is defined over a discrete label space and may vary arbitrarily across classes, without any continuity or monotonicity constraints. This discreteness induces nontrivial, instance-dependent conformal p-value distributions. As a result, EPU quantification in classification captures genuine differences in how compatible a test instance x is with the calibration set.

In regression, by contrast, most commonly used nonconformity scores are typically continuous in y and monotone in the distance from a central prediction¹. Under such constructions, the critical

¹Specifically, constructing conformal prediction regions via posterior predictive level sets (Fong & Holmes, 2021) may circumvent this issue; however, due to scope limitations, we leave a detailed investigation to future work.

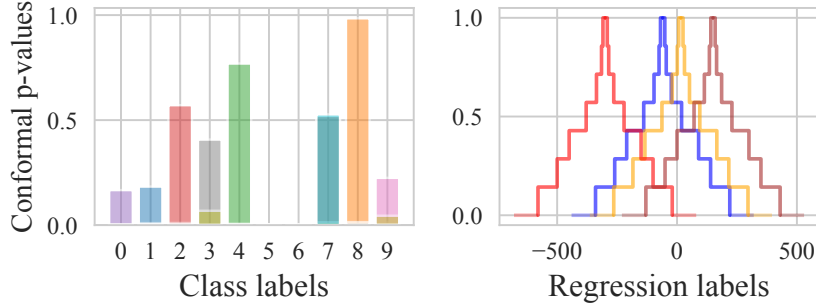


Figure 3: Conformal p-value portfolio for classification and regression, where each colour represents a different test instance. While conformal classification exhibits instance-specific p-value distributions, conformal regression yields distributions with identical shapes across instances.

quantities appearing in Propositions 3.6 and 3.8 reduce to constants determined solely by the calibration data. Consequently, the induced EPU is invariant across test instances.

In summary, classification admits instance-specific conformal p-value distributions due to label-space discreteness, whereas in regression, continuity and monotonicity of the score function eliminate test-specific variability. Figure 3 illustrates this effect. By Proposition 3.4, conformal p-values define an implicit predictive credal set; identical p-value distributions therefore induce identical credal sets, implying that any credal-set-based EPU measure assigns the same value to all test instances. For this reason, since common conformal regression provides no informative signal for distinguishing test instances, we do not include regression experiments.

3.3 Discussion on the consonance assumption

The consonance assumption provides a bridge between CP and IP, enabling EPU to be quantified via the amount of conflict encoded within the induced predictive credal set. Nonetheless, this naturally raises the question of how such a modification affects the underlying conformal procedure. We answer this with the following propositions.

Proposition 3.9. *Let $\tilde{\pi}_x$ be the modified consonant transducer from the original transducer π_x . Let $\tilde{C}_\alpha(\cdot)$ be the CPR constructed using $\tilde{\pi}_x$. Then, for any test instances x , it is true that*

1. we have

$$\tilde{C}_\alpha(x) \setminus C_\alpha(x) = \{y_{\sigma(1)}\}$$

if and only if $C_\alpha(x) = \emptyset$, otherwise

$$\tilde{C}_\alpha(x) = C_\alpha(x).$$

2. For prediction on unseen data (X_{n+1}, Y_{n+1}) , the marginal coverage guarantee is preserved, i.e.

$$\mathbb{P}(Y_{n+1} \in \tilde{C}_\alpha(X_{n+1})) \geq 1 - \alpha.$$

Proposition 3.9 implies that the stretched transducer enlarges the prediction set only when the original prediction set is empty; otherwise, the two sets coincide. Moreover, the marginal coverage guarantee is preserved. Consequently, enforcing consonance precludes conformal prediction from producing empty prediction sets, thereby removing its ability to explicitly signal extreme predictive

uncertainty in rare or highly atypical prediction scenarios. While we acknowledge this limitation, we emphasise that enforcing consonance in return yields a stronger statistical guarantee than marginal coverage alone, as we show below.

Theorem 3.10 (Uniform validity of consonance conformal prediction (Cella & Martin, 2022)). *Consonance conformal transducers yield a conformal procedure that is uniformly valid, that is*

$$\mathbb{P}(\pi_{X_{n+1}}(Y_{n+1}) \leq \alpha) \leq \alpha,$$

for all n and exchangeable \mathbb{P} . Moreover, uniform validity is equivalent to satisfying

$$\mathbb{P}\left(\left\{\overline{\mathbb{P}_{X_{n+1}}}(A) \leq \alpha \text{ and } Y_{n+1} \in A \text{ for some } A\right\}\right) \leq \alpha$$

for all n, α and exchangeable \mathbb{P} .

This condition is strictly stronger than the marginal coverage guarantee of standard conformal prediction, in the sense that the former implies the latter; see Cella & Martin (2022, Proposition 2) for details. Intuitively, this result goes beyond coverage guarantees: enforcing consonance allows us to guarantee the reliability of the resulting implicit probabilistic predictors. In particular, when the upper probability $\overline{\mathbb{P}}_x$ assigns low plausibility to an event $Y_{n+1} \in A$, the actual probability that $Y_{n+1} \in A$ occurs is also small.

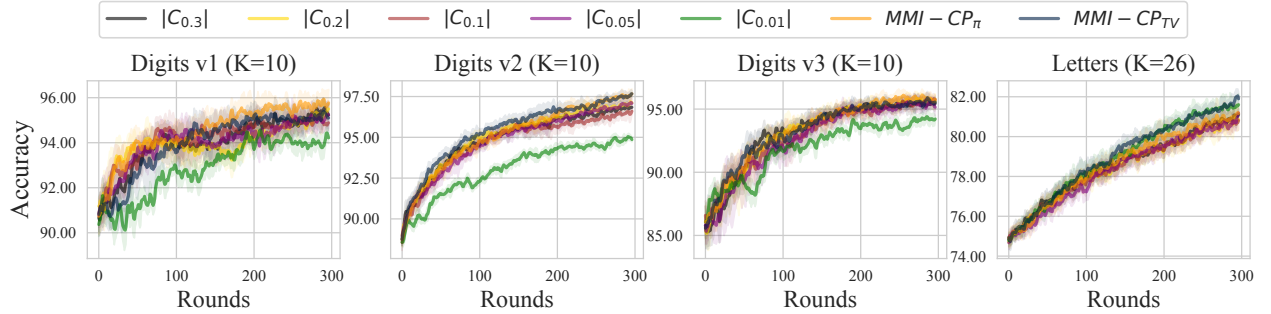
Overall, enforcing consonance entails a trade-off of expressive power, in that empty prediction sets are no longer permitted, but it otherwise preserves the conformal procedure and upgrades the associated statistical guarantee from marginal coverage to Type II validity.

4 Related Work

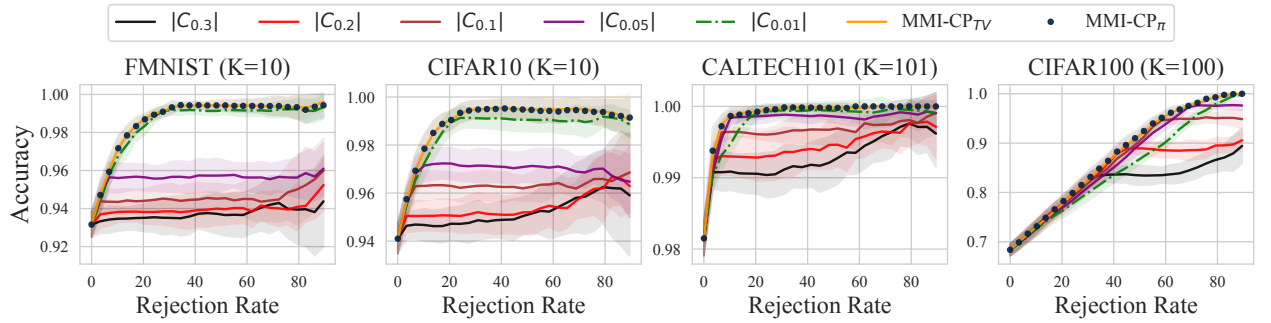
CP and epistemic uncertainty. On the topic of conformal prediction (CP) and epistemic uncertainty, Karimi & Samavi (2023) proposed a heuristic normalisation of CPR sizes at fixed α to $[0, 1]$ based on the calibration set size. Since this transformation preserves the instance-wise ranking induced solely by CPR sizes, it does not affect ranking-based decision rules; we therefore omit it from our experiments. Javanmardi et al. (2025) incorporated second-order predictions into CP, and Cabezas et al. (2025) incorporated the EPU of a general predictive model into score design; in contrast, we study the EPU induced by the conformal procedure itself. In a related but orthogonal direction, Caprio et al. (2025d) and Javanmardi et al. (2024) studied conformal classification with ambiguous (distribution-valued) labels rather than one-hot encodings, resulting in predictive credal sets with conformal-like guarantees; by contrast, we characterise the credal set induced by an arbitrary CP procedure.

5 Experiments

This section demonstrates the practical utility of our proposed MMI-CP methods. Since ground-truth EPU does not exist, the informativeness of EPU measures is commonly assessed through their effectiveness in supporting downstream decision-making. We therefore conduct two sets of experiments—active learning and selective classification—to evaluate the advantages of our methods over relying on CPR sizes. We denote our MMI-based approaches as MMI-CP_{TV} (Proposition 3.5) and MMI-CP _{π_x} (Proposition 3.6), and compare against CPR sizes $|C_\alpha|$ at confidence levels $\alpha \in \{0.01, 0.05, 0.10, 0.20, 0.30\}$. For both experiments, we use the most probable outcome from \hat{f} to make point prediction, while using conformal procedures to extract the conformal p-values to either



(a) Accuracies of the predictive model at each active learning round.



(b) The accuracy-rejection curve for selective classification experiments.

Figure 4: Results averaged over 10 seeds and 1 standard error reported. In general, MMI-based approaches outperform the set-size-based approaches, suggesting that the former provide more fine-grained epistemic uncertainty information for downstream decision-making.

Table 1: Experiment results: \dagger/\star denote statistically significantly worse performance than $\text{MMI-CP}_{\pi_x}/\text{MMI-CP}_{\text{TV}}$, respectively (Wilcoxon signed-rank test, 5%). Results are averaged over 10 seeds; one standard error is reported.

(a) (Active learning) Accuracies achieved at the final step.

	Digits v1	Digits v2	Digits v3	Letters
# classes	10	10	10	26
MMI-CP _{TV}	$95.30 \pm 0.29^\dagger$	97.69 ± 0.29	95.75 ± 0.47	82.00 ± 0.39
MMI-CP _{π_x}	95.80 ± 0.40	97.83 ± 0.42	95.90 ± 0.41	81.40 ± 0.61
$ C_{0.01}(\cdot) $	94.00 ± 0.22	$94.91 \pm 0.14^\dagger\star$	$94.30 \pm 0.40^\dagger\star$	$81.32 \pm 0.33^\dagger\star$
$ C_{0.05}(\cdot) $	95.30 ± 0.53	$97.01 \pm 0.14^\dagger\star$	$94.90 \pm 0.51^\dagger$	$80.86 \pm 0.17^\dagger\star$
$ C_{0.1}(\cdot) $	$95.05 \pm 0.53^\dagger$	$96.74 \pm 0.40^\dagger\star$	$95.85 \pm 0.34^\dagger$	80.75 ± 0.85
$ C_{0.2}(\cdot) $	$95.40 \pm 0.25^\dagger$	$97.01 \pm 0.28^\dagger\star$	95.80 ± 0.19	81.10 ± 0.41
$ C_{0.3}(\cdot) $	$95.40 \pm 0.64^\dagger$	$96.90 \pm 0.23^\dagger\star$	95.55 ± 0.80	81.05 ± 0.27

(b) (Selective classification) Area under ARC.

	Cifar10	Cifar100	Caltech	FMNIST
# classes	10	100	100	10
MMI-CP _{TV}	97.34 ± 1.42	88.16 ± 0.87	98.53 ± 0.03	97.54 ± 0.27
MMI-CP _{π_x}	97.68 ± 0.46	88.28 ± 0.91	98.53 ± 0.03	$97.52 \pm 0.29^\star$
$ C_{0.01}(\cdot) $	$97.37 \pm 0.43^\dagger$	$85.92 \pm 0.94^\dagger\star$	$98.43 \pm 0.14^\dagger\star$	97.29 ± 0.29
$ C_{0.05}(\cdot) $	$95.66 \pm 0.62^\dagger\star$	$86.81 \pm 1.01^\dagger\star$	$98.43 \pm 0.08^\dagger\star$	$94.39 \pm 0.76^\dagger\star$
$ C_{0.1}(\cdot) $	$95.15 \pm 0.52^\dagger\star$	$86.36 \pm 1.16^\dagger\star$	$98.30 \pm 0.14^\dagger\star$	$93.59 \pm 0.86^\star$
$ C_{0.2}(\cdot) $	$94.30 \pm 0.83^\dagger\star$	$83.19 \pm 2.11^\dagger\star$	$98.09 \pm 0.22^\dagger\star$	$93.00 \pm 0.58^\star$
$ C_{0.3}(\cdot) $	$93.73 \pm 1.74^\dagger\star$	$81.53 \pm 1.97^\dagger\star$	$97.95 \pm 0.24^\dagger\star$	$92.69 \pm 1.09^\dagger\star$

compute the relevant MMI measures or the conformal set sizes. Due to space constraints, full experimental details, statistical significance tests, and ablation studies on how choices of score functions and the calibration set sizes affect our results are provided in Appendix D. All experiments are repeated over 10 random seeds, and the code is available at [Anonymous \(2026\)](#).

Active learning. Following [Nguyen et al. \(2022\)](#) and [Thomas & Houssineau \(2024\)](#), we evaluate the informativeness of the proposed approaches by their ability to select the next data point to query that most effectively improves learning. Informative EPU measures should identify instances whose labels’ acquisition reduces predictive ambiguity the most, making active learning performance a practical proxy for EPU quality. We conduct experiments on four datasets from the OpenML repository ([Vanschoren et al., 2014](#)), comprising three datasets with 10 classes and one dataset with 26 classes. In all experiments, we use a random forest classifier as the base learner, and the adaptive prediction sets score (APS) ([Romano et al., 2020](#)) as the nonconformity score. At each round, we train a random forest model on 70% of the training data, evaluate its accuracy on a separate and fixed held-out test set, and compute EPU measures via the conformal procedure using the remaining 30% calibration data. We then select the most epistemically uncertain instance from the unlabelled pool, query its label, augment the training set, and repeat this process for 300 rounds.

Results. Figure 4a presents accuracy trajectories during active learning, and Table 1a reports the final-round accuracy. Overall, the MMI-based methods, especially MMI-CP_{π_x} , consistently achieve higher performance on average and, in many cases, statistically significantly outperform the fixed α set-size-based methods. We observe no systematic trend with respect to the choice of the tolerance

level α : in some cases, smaller values of α yield better performance, while in others larger values perform better. As the number of classes increases, prediction set sizes can take a wider range of values and may therefore become more informative. Consistent with this intuition, the performance gap between set-size-based methods and MMI-based methods narrows in higher-class problems. Nevertheless, even in these settings, α set-size-based methods still underperform relative to their MMI-based counterparts.

Selective classification. Next, following Shaker & Hüllermeier (2021) and Chau et al. (2025), we evaluate the proposed approaches by their ability to rank test instances according to their prediction difficulty. Specifically, we consider the accuracy-rejection curve (ARC), which plots predictive accuracy as a function of the rejection rate. An ideal uncertainty-aware model that abstains on the most uncertain $p\%$ of inputs and predicts on the remaining $(1 - p)\%$ should exhibit increasing accuracy as p increases. Consequently, an informative EPU measure that reliably identifies confident instances should produce a non-decreasing ARC that approaches the top-left corner of the plot. We conduct experiments on four standard benchmark datasets—CIFAR10, CIFAR100, Caltech101, and FMNIST—of which two have 10 classes, and two have 100 classes. We use pretrained deep neural networks from PyTorch (Paszke et al., 2019) and Hugging Face as predictive models and, as before, employ the adaptive prediction set score as the nonconformity score. The calibration set is obtained from a subset of the withheld data, and the remaining samples are used to compute accuracy on a held-out test set of size 1000 samples.

Results. Figure 4b and Table 1b present the ARCs and the area under ARCs, respectively. Consistent with the active learning results, the MMI-based approaches—on average and in most cases significantly—outperform the set-size-based methods. We also observe a similar trend with respect to the number of classes: as the number of classification labels increases, the performance gap between set-size-based approaches and MMI-based methods narrows, although MMI-based approaches remain superior. While smaller values of α often appear to yield more discriminative EPU proxies in ARC-based evaluations, this trend does not carry over to the active learning setting. In fact, smaller α can lead to inferior active learning performance. This discrepancy suggests that there is no universally optimal choice of α for acting as a proxy for EPU, and that the optimal choice is problem-dependent. In contrast, the MMI-based methods, grounded in rigorous theoretical analysis, exhibit robust performance across different evaluation settings.

6 Discussion

We study the problem of quantifying epistemic predictive uncertainty in conformal prediction by proving that (split) CP implicitly defines an imprecise probabilistic predictor and leverage this insight to adapt the general MMI framework to the conformal setting, yielding analytically tractable and computationally efficient uncertainty measures. Experiments on active learning and selective prediction demonstrate improved practical performance on EPU quantification in conformal classification. We also identify fundamental limitations for quantifying EPU in conformal regression. We argue that these negative results reflect intrinsic properties of standard conformal regression rather than shortcomings of our approach.

In future work, we will extend our framework to quantifying epistemic uncertainty for other conformal settings, such as conformal decision-making (Vovk & Bendtsen, 2018), or conformal prediction for time series and online learning problems (Sale & Ramdas, 2025).

Further discussion of the interpretations of our results and the technical background is provided in

Appendices A and B.

References

Abellán, J. and Klir, G. J. Additivity of uncertainty measures on credal sets. *International Journal of General Systems*, 34(6):691–713, 2005.

Abellán, J. and Gómez, M. Measures of divergence on credal sets. *Fuzzy Sets and Systems*, 157(11): 1514–1531, June 2006. ISSN 01650114. doi: 10.1016/j.fss.2005.11.021.

Abellán, J., Klir, G. J., and Moral, S. Disaggregated total uncertainty measure for credal sets. *International Journal of General Systems*, 1(35):29–44, 2006.

Alpaydin, E. and Kaynak, C. Cascading classifiers. *Kybernetika*, 1998.

Angelopoulos, A. N., Bates, S., Jordan, M., and Malik, J. Uncertainty sets for image classifiers using conformal prediction. In *International Conference on Learning Representations*, 2021.

Anonymous. Anonymous repository for conformalmmi experiments. <https://anonymous.4open.science/r/ConformalMMI-1244/>, 2026. Code and experimental details for reproducibility (anonymous for double-blind review).

Augustin, T., Coolen, F. P. A., De Cooman, G., and Troffaes, M. C. M. (eds.). *Introduction to imprecise probabilities*. Wiley series in probability and statistics. Wiley, Hoboken, NJ, 2014. ISBN 978-0-470-97381-3.

Balasubramanian, V., Ho, S.-S., and Vovk, V. *Conformal prediction for reliable machine learning: theory, adaptations and applications*. Newnes, 2014.

Baron, J. Second-order probabilities and belief functions. *Theory and Decision*, 23(1):25–36, 1987.

Bertrand, J. *Calcul des probabilités*. Gauthier-Villars, 1889.

Boström, H. and Johansson, U. Mondrian conformal regressors. In *Conformal and probabilistic prediction and applications*, pp. 114–133. PMLR, 2020.

Cabezas, L. M. C., Santos, V. S., Ramos, T., and Izbicki, R. Epistemic uncertainty in conformal scores: A unified approach. In *The 41st Conference on Uncertainty in Artificial Intelligence*, 2025.

Campos, M. M., Cálem, J., Sklaviadis, S., Figueiredo, M. A., and Martins, A. Sparse activations as conformal predictors. In *International Conference on Artificial Intelligence and Statistics*, pp. 2674–2682. PMLR, 2025.

Caprio, M. Optimal transport for ϵ -contaminated credal sets. In Destercke, S., Erreygers, A., Nendel, M., Riedel, F., and Troffaes, M. C. M. (eds.), *Proceedings of the Fourteenth International Symposium on Imprecise Probabilities: Theories and Applications*, volume 290 of *Proceedings of Machine Learning Research*, pp. 33–46. PMLR, 15–18 Jul 2025a. URL <https://proceedings.mlr.press/v290/caprio25a.html>.

Caprio, M. The joys of categorical conformal prediction, 2025b. URL <https://arxiv.org/abs/2507.04441>.

Caprio, M. and Gong, R. Dynamic precise and imprecise probability kinematics. In Miranda, E., Montes, I., Quaeghebeur, E., and Vantaggi, B. (eds.), *Proceedings of the Thirteenth International Symposium on Imprecise Probability: Theories and Applications*, volume 215 of *Proceedings of Machine Learning Research*, pp. 72–83. PMLR, 11–14 Jul 2023.

Caprio, M. and Mukherjee, S. Ergodic theorems for dynamic imprecise probability kinematics. *International Journal of Approximate Reasoning*, 152:325–343, 2023.

Caprio, M. and Seidenfeld, T. Constriction for sets of probabilities. In Miranda, E., Montes, I., Quaeghebeur, E., and Vantaggi, B. (eds.), *Proceedings of the Thirteenth International Symposium on Imprecise Probability: Theories and Applications*, volume 215 of *Proceedings of Machine Learning Research*, pp. 84–95. PMLR, 11–14 Jul 2023. URL <https://proceedings.mlr.press/v215/caprio23b.html>.

Caprio, M., Dutta, S., Jang, K. J., Lin, V., Ivanov, R., Sokolsky, O., and Lee, I. Credal bayesian deep learning. *Transactions on Machine Learning Research*, 2024a. ISSN 2835-8856. URL <https://openreview.net/forum?id=4NHF9AC5ui>.

Caprio, M., Sale, Y., Hüllermeier, E., and Lee, I. A Novel Bayes’ Theorem for Upper Probabilities. In Cuzzolin, F. and Sultana, M. (eds.), *Epistemic Uncertainty in Artificial Intelligence*, pp. 1–12, Cham, 2024b. Springer Nature Switzerland.

Caprio, M., Sultana, M., Elia, E., and Cuzzolin, F. Credal learning theory. In *The Thirty-eighth Annual Conference on Neural Information Processing Systems*, 2024c. URL <https://openreview.net/forum?id=AH5KwUSsln>.

Caprio, M., Chau, S. L., and Muandet, K. When do credal sets stabilize? fixed-point theorems for credal set updates. *arXiv preprint arXiv:2510.04769*, 2025a.

Caprio, M., Manchingal, S. K., and Cuzzolin, F. Credal and interval deep evidential classifications, 2025b. URL <https://arxiv.org/abs/2512.05526>.

Caprio, M., Sale, Y., and Hüllermeier, E. Conformal prediction regions are imprecise highest density regions. In Destercke, S., Erreygers, A., Nendel, M., Riedel, F., and Troffaes, M. C. M. (eds.), *Proceedings of the Fourteenth International Symposium on Imprecise Probabilities: Theories and Applications*, volume 290 of *Proceedings of Machine Learning Research*, pp. 47–59. PMLR, 15–18 Jul 2025c. URL <https://proceedings.mlr.press/v290/caprio25b.html>.

Caprio, M., Stutz, D., Li, S., and Doucet, A. Conformalized credal regions for classification with ambiguous ground truth. *Transactions on Machine Learning Research*, 2025d.

Cella, L. and Martin, R. Validity, consonant plausibility measures, and conformal prediction. *International Journal of Approximate Reasoning*, 141:110–130, 2022. Probability and Statistics: Foundations and History. In honor of Glenn Shafer.

Cerreia-Vioglio, S., Maccheroni, F., and Marinacci, M. Ergodic theorems for lower probabilities. *Proceedings of the American Mathematical Society*, 144(8):3381–3396, 2016.

Chau, S. L., Muandet, K., and Sejdinovic, D. Explaining the uncertain: Stochastic shapley values for gaussian process models. *Advances in Neural Information Processing Systems*, 36:50769–50795, 2023.

Chau, S. L., Schrab, A., Gretton, A., Sejdinovic, D., and Muandet, K. Credal two-sample tests of epistemic ignorance. *arXiv preprint arXiv:2410.12921*, 2024.

Chau, S. L., Caprio, M., and Muandet, K. Integral imprecise probability metrics. In *The Thirty-ninth Annual Conference on Neural Information Processing Systems*, 2025. URL <https://openreview.net/forum?id=KM2XzHq2Rm>.

Choquet, G. Théorie des capacités. *Ann. Inst. Fourier 5 (1953/1954) 131–292.*, 1953.

Coolen, F. P. A. Imprecise highest density regions related to intervals of measures. *Memorandum COSOR*, 9254, 1992.

Cortes, C., DeSalvo, G., and Mohri, M. Learning with rejection. In *International conference on algorithmic learning theory*, pp. 67–82. Springer, 2016.

Cozman, F. G. Credal networks. *Artificial intelligence*, 120(2):199–233, 2000.

Cuzzolin, F. *The geometry of uncertainty: the geometry of imprecise probabilities*. Springer Nature, 2020.

Cuzzolin, F. and Frezza, R. Evidential reasoning framework for object tracking. In *Telemanipulator and Telepresence Technologies VI*, volume 3840, pp. 13–24. SPIE, 1999.

De Cooman, G. Possibility theory I: the measure-and integral-theoretic groundwork. *International Journal of General Systems*, 25(4):291–323, 1997.

Denoeux, T. A neural network classifier based on dempster-shafer theory. *IEEE Transactions on Systems, Man, and Cybernetics-Part A: Systems and Humans*, 30(2):131–150, 2000.

Destercke, S. Handling bipolar knowledge with credal sets. In *Combining Soft Computing and Statistical Methods in Data Analysis*, pp. 199–207. Springer, 2010.

Dubois, D. and Hüllermeier, E. Comparing probability measures using possibility theory: A notion of relative peakedness. *International Journal of Approximate Reasoning*, 45(2):364–385, 2007. Eighth European Conference on Symbolic and Quantitative Approaches to Reasoning with Uncertainty (ECSQARU 2005).

Dubois, D. and Prade, H. Théorie des possibilités, 1985.

Dutta, S., Caprio, M., Lin, V., Cleaveland, M., Jang, K. J., Ruchkin, I., Sokolsky, O., and Lee, I. Distributionally robust statistical verification with imprecise neural networks. In *Proceedings of the 28th ACM International Conference on Hybrid Systems: Computation and Control*, HSCC '25, New York, NY, USA, 2025. Association for Computing Machinery. ISBN 9798400715044. doi: 10.1145/3716863.3718040. URL <https://doi.org/10.1145/3716863.3718040>.

Fei-Fei, L., Fergus, R., and Perona, P. Learning generative visual models from few training examples. In *Proceedings of the IEEE Conference on Computer Vision and Pattern Recognition (CVPR)*, 2004.

Fong, E. and Holmes, C. C. Conformal bayesian computation. *Advances in Neural Information Processing Systems*, 34:18268–18279, 2021.

Frey, P. W. and Slate, D. J. Letter recognition using holland-style adaptive classifiers. *Machine Learning*, 6(2):161–182, 1991.

Friedman, N. and Halpern, J. Y. Plausibility measures: a user's guide. In *Proceedings of the Eleventh conference on Uncertainty in artificial intelligence*, pp. 175–184, 1995.

Fröhlich, C. and Williamson, R. C. Scoring rules and calibration for imprecise probabilities. *arXiv preprint arXiv:2410.23001*, 2024.

Gaifman, H. A theory of higher order probabilities. In *Theoretical aspects of reasoning about knowledge*, pp. 275–292. Elsevier, 1986.

Gal, Y. et al. Uncertainty in deep learning. 2016.

Giunchiglia, E., Stoian, M. C., Khan, S., Cuzzolin, F., and Lukasiewicz, T. Road-r: the autonomous driving dataset with logical requirements. *Machine Learning*, 112(9):3261–3291, 2023.

Hartley, R. V. Transmission of information 1. *Bell System technical journal*, 7(3):535–563, 1928.

Hofman, P., Sale, Y., and Hüllermeier, E. Quantifying aleatoric and epistemic uncertainty: A credal approach. In *ICML 2024 Workshop on Structured Probabilistic Inference \& Generative Modeling*, 2024.

Huang, J., Song, J., Zhou, X., Jing, B., and Wei, H. Torchcp: A python library for conformal prediction, 2024.

Hyndman, R. J. Computing and graphing highest density regions. *The American Statistician*, 50(2):120–126, 1996.

Hájek, A. Interpretations of Probability. In Zalta, E. N. (ed.), *The Stanford Encyclopedia of Philosophy*. Metaphysics Research Lab, Stanford University, fall 2019 edition, 2019. URL <https://plato.stanford.edu/archives/fall2019/entries/probability-interpret/>.

Hüllermeier, E. and Waegeman, W. Aleatoric and Epistemic Uncertainty in Machine Learning: An Introduction to Concepts and Methods. *Machine Learning*, 110(3):457–506, March 2021. ISSN 0885-6125, 1573-0565. doi: 10.1007/s10994-021-05946-3. arXiv:1910.09457 [cs, stat].

Jain, A. K., Duin, R. P. W., and Mao, J. Statistical pattern recognition: A review. *IEEE Transactions on pattern analysis and machine intelligence*, 22(1):4–37, 2000.

Javanmardi, A., Stutz, D., and Hüllermeier, E. Conformalized credal set predictors. *Advances in Neural Information Processing Systems*, 37:116987–117014, 2024.

Javanmardi, A., Zargarbashi, S. H., Thies, S. M., Waegeman, W., Bojchevski, A., and Hüllermeier, E. Optimal conformal prediction under epistemic uncertainty. *arXiv preprint arXiv:2505.19033*, 2025.

Jürgens, M., Mortier, T., Hüllermeier, E., Bengs, V., and Waegeman, W. A calibration test for evaluating set-based epistemic uncertainty representations. *arXiv preprint arXiv:2502.16299*, 2025.

Karimi, H. and Samavi, R. Quantifying deep learning model uncertainty in conformal prediction. In *Proceedings of the AAAI Symposium Series*, volume 1, pp. 142–148, 2023.

Kendall, A. and Gal, Y. What uncertainties do we need in bayesian deep learning for computer vision? *Advances in neural information processing systems*, 30, 2017.

Keynes, J. M. *A treatise on probability*. 1921.

Kingman, J. G. matheron, random sets and integral geometry. 1975.

Knight, F. H. *Risk, uncertainty and profit*, volume 31. Houghton Mifflin, 1921.

Kolmogorov. Sulla determinazione empirica di una legge didistribuzione. *Giorn Dell'inst Ital Degli Att*, 4:89–91, 1933.

Krizhevsky, A. and Hinton, G. Learning multiple layers of features from tiny images. Technical report, 2009.

Levi, I. *The Enterprise of Knowledge*. London, UK : MIT Press, 1980.

Liell-Cock, J. and Staton, S. Compositional imprecise probability: A solution from graded monads and markov categories. 9(POPL), 2025. doi: 10.1145/3704890. URL <https://doi.org/10.1145/3704890>.

Löfström, T., Boström, H., Linusson, H., and Johansson, U. Bias reduction through conditional conformal prediction. *Intelligent Data Analysis*, 19(6):1355–1375, 2015.

Lu, P., Caprio, M., Eaton, E., and Lee, I. IBCL: Zero-shot Model Generation for Task Trade-offs in Continual Learning. *arXiv preprint arXiv:2305.14782*, 2025.

Madras, D., Pitassi, T., and Zemel, R. Predict responsibly: improving fairness and accuracy by learning to defer. *Advances in neural information processing systems*, 31, 2018.

Marinacci, M. and Montrucchio, L. Introduction to the mathematics of ambiguity. In Gilboa, I. (ed.), *Uncertainty in economic theory: a collection of essays in honor of David Schmeidler's 65th birthday*. London : Routledge, 2004.

Martin, R. An efficient monte carlo method for valid prior-free possibilistic statistical inference, 2025. URL <https://arxiv.org/abs/2501.10585>.

Mohammadi, M., Muandet, K., Tiddi, I., Teije, A. T., and Chau, S. L. Exact shapley attributions in quadratic-time for fanova gaussian processes. *AAAI*, 2026.

Müller, A. Integral probability metrics and their generating classes of functions. *Advances in applied probability*, 29(2):429–443, 1997.

Nguyen, V.-L., Shaker, M. H., and Hüllermeier, E. How to measure uncertainty in uncertainty sampling for active learning. *Machine Learning*, 111:89–122, 2022.

Papadopoulos, H., Proedrou, K., Vovk, V., and Gammerman, A. Inductive confidence machines for regression. In *European conference on machine learning*, pp. 345–356. Springer, 2002.

Paszke, A., Gross, S., Massa, F., Lerer, A., Bradbury, J., Chanan, G., Killeen, T., Lin, Z., Gimelshein, N., Antiga, L., et al. Pytorch: An imperative style, high-performance deep learning library. *Advances in neural information processing systems*, 32, 2019.

Romano, Y., Sesia, M., and Candes, E. Classification with valid and adaptive coverage. *Advances in neural information processing systems*, 33:3581–3591, 2020.

Sale, Y. and Ramdas, A. Online selective conformal inference: Errors and solutions. *Transactions on Machine Learning Research*, 2025.

Sale, Y., Caprio, M., and Höllermeier, E. Is the volume of a credal set a good measure for epistemic uncertainty? In *Uncertainty in Artificial Intelligence*, pp. 1795–1804. PMLR, 2023.

Sale, Y., Bengs, V., Caprio, M., and Hüllermeier, E. Second-order uncertainty quantification: A distance-based approach. In Salakhutdinov, R., Kolter, Z., Heller, K., Weller, A., Oliver, N., Scarlett, J., and Berkenkamp, F. (eds.), *Proceedings of the 41st International Conference on Machine Learning*, volume 235 of *Proceedings of Machine Learning Research*, pp. 43060–43076. PMLR, 21–27 Jul 2024. URL <https://proceedings.mlr.press/v235/sale24a.html>.

Sale, Y., Javanmardi, A., and Hüllermeier, E. Aleatoric and epistemic uncertainty in conformal prediction. In *Fourteenth Symposium on Conformal and Probabilistic Prediction with Applications (COPA 2025)*, pp. 784–786. PMLR, 2025.

Settles, B. Active learning literature survey. 2009.

Shafer, G. *A mathematical theory of evidence*, volume 42. Princeton university press, 1976.

Shafer, G. and Vovk, V. A tutorial on conformal prediction. *Journal of Machine Learning Research*, 9:371–421, 2008.

Shahriari, B., Swersky, K., Wang, Z., Adams, R. P., and De Freitas, N. Taking the human out of the loop: A review of bayesian optimization. *Proceedings of the IEEE*, 104(1):148–175, 2015.

Shaker, M. H. and Hüllermeier, E. Ensemble-based uncertainty quantification: Bayesian versus credal inference. In *Proceedings 31. workshop computational intelligence*, volume 25, pp. 63, 2021.

Singh, A., Chau, S. L., Bouabid, S., and Muandet, K. Domain generalisation via imprecise learning. In *International Conference on Machine Learning*, pp. 45544–45570. PMLR, 2024.

Singh, A., Chau, S. L., and Muandet, K. Truthful elicitation of imprecise forecasts. In *The 41st Conference on Uncertainty in Artificial Intelligence*, 2025a.

Singh, A., Chau, S. L., and Muandet, K. Truthful elicitation of imprecise forecasts. In *The 41st Conference on Uncertainty in Artificial Intelligence*, 2025b.

Sloman, S. J., Caprio, M., and Kaski, S. Epistemic errors of imperfect multitask learners when distributions shift, 2025. URL <https://arxiv.org/abs/2505.23496>.

Stone, J. V. Information theory: A tutorial introduction to the principles and applications of information theory. 2024.

Stutz, D., Roy, A. G., Matejovicova, T., Strachan, P., Cemgil, A. T., and Doucet, A. Conformal prediction under ambiguous ground truth. *arXiv preprint arXiv:2307.09302*, 2023.

Sugeno, M. Theory of fuzzy integrals and its applications. *Doctoral Thesis, Tokyo Institute of Technology*, 1974.

Thomas, J. and Houssineau, J. Improving active learning with a bayesian representation of epistemic uncertainty. *arXiv preprint arXiv:2412.08225*, 2024.

Troffaes, M. C. and de Cooman, G. *Lower Previsions*. Chichester, United Kingdom : John Wiley and Sons, 2014.

Utkin, L., Konstantinov, A., Vishniakov, K., and Ilin, I. Imprecise shap as a tool for explaining the class probability distributions under limited training data. In *Digital Systems and Information Technologies in the Energy Sector*, pp. 369–389. Springer, 2025.

Vanschoren, J., Van Rijn, J. N., Bischl, B., and Torgo, L. Openml: networked science in machine learning. *ACM SIGKDD Explorations Newsletter*, 15(2):49–60, 2014.

Vovk, V. and Bendtsen, C. Conformal predictive decision making. In *Conformal and Probabilistic Prediction and Applications*, pp. 52–62. PMLR, 2018.

Walley, P. *Statistical Reasoning with Imprecise Probabilities*, volume 42 of *Monographs on Statistics and Applied Probability*. London : Chapman and Hall, 1991.

Wang, K., Cuzzolin, F., Shariatmadar, K., Moens, D., Hallez, H., et al. Credal deep ensembles for uncertainty quantification. *Advances in Neural Information Processing Systems*, 37:79540–79572, 2024.

Wang, K., Cuzzolin, F., Shariatmadar, K., Moens, D., and Hallez, H. Credal wrapper of model averaging for uncertainty estimation in classification. In *The Thirteenth International Conference on Learning Representations*, 2025a.

Wang, K., Shariatmadar, K., Manchingal, S. K., Cuzzolin, F., Moens, D., and Hallez, H. Creinns: Credal-set interval neural networks for uncertainty estimation in classification tasks. *Neural Networks*, 185:107198, 2025b. ISSN 0893-6080. doi: <https://doi.org/10.1016/j.neunet.2025.107198>. URL <https://www.sciencedirect.com/science/article/pii/S0893608025000772>.

Williamson, J. *In defence of objective Bayesianism*. OUP Oxford, 2010.

Xiao, H., Rasul, K., and Vollgraf, R. Fashion-mnist: a novel image dataset for benchmarking machine learning algorithms. *arXiv preprint arXiv:1708.07747*, 2017.

Zaffalon, M. Exact credal treatment of missing data. *Journal of statistical planning and inference*, 105(1):105–122, 2002.

Zaffalon, M., Antonucci, A., Cabañas, R., and Huber, D. Approximating counterfactual bounds while fusing observational, biased and randomised data sources. *International Journal of Approximate Reasoning*, 162:109023, 2023.

Contents

A Further discussions on concepts and interpretations.	23
A.1 Analogy to Bayesian predictions and interpretation of uncertainty	23
A.1.1 Bayesian Probabilistic Prediction.	23
A.1.2 Conformal Prediction	25
A.2 Is the credal set perspective necessary?	26
A.3 How is the epistemic uncertainty discussed here differ from the one in Sale et al. (2025) ? .	26
B Background on Imprecise Probabilities and Imprecise Probabilistic Machine Learning	28
B.1 Imprecise Probabilities	28
B.2 Imprecise Probabilistic Machine Learning	28
B.3 Credal Uncertainty Quantification Measures and MMI	29
B.3.1 Maximum Mean Imprecision (Chau et al., 2025)	30
C Proofs and derivations	31
C.1 Proof for Proposition 3.2	31
C.2 Proof for Proposition 3.4	31
C.3 Proof for Proposition 3.5	32
C.4 Proof for Proposition 3.6	32
C.5 Proof for Proposition 3.7	33
C.6 Proof for Proposition 3.8	34
C.7 Proof for Proposition 3.9	35
C.8 Proof for Theorem 3.10	36
D Experimental details and further ablation studies	37
D.1 Statistical Significance tables	38
D.2 Ablation study on the choice of nonconformity scores	40
D.3 Ablation study on the sizes of the calibration set	41

A Further discussions on concepts and interpretations.

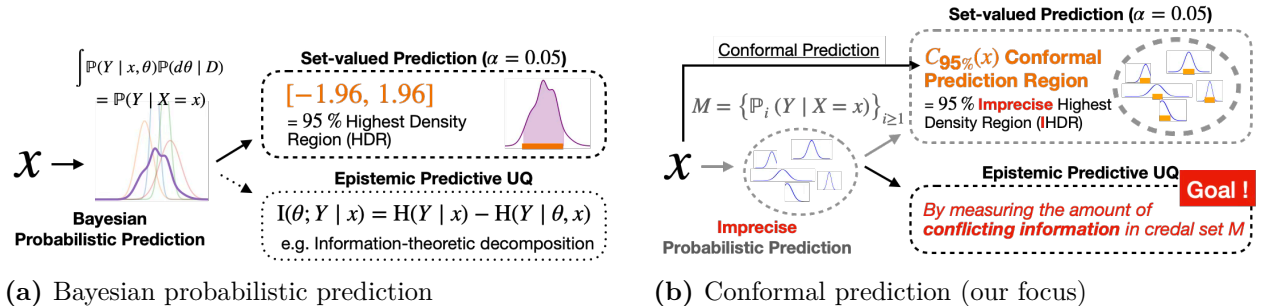
We include this section in the appendix to provide additional exposition of several concepts that are only briefly mentioned in the main text due to space constraints.

A.1 Analogy to Bayesian predictions and interpretation of uncertainty

As the problem of quantifying epistemic predictive uncertainty in conformal prediction is relatively new, we devote this subsection to a deeper discussion of the introduced concepts, with particular emphasis on what types of uncertainty are being quantified and at which stage they arise. To facilitate this discussion, we draw an analogy with the Bayesian prediction paradigm. In particular, rather than adopting the standard aleatoric-epistemic dichotomy, we instead pose a different question: what do the various quantified uncertainties actually describe, and to which components of the prediction process are they associated?

*In simple words, what really matters here is to differentiate between uncertainty associated with **making a prediction** from uncertainty associated with the **prediction itself**. For instance, epistemic predictive uncertainty describes the uncertainty associated with the former, and measuring prediction set sizes describes the uncertainty associated with the latter.*

As these concepts are rarely discussed in depth in machine learning, drawing an analogy to Bayesian predictions could be more insightful.



A.1.1 Bayesian Probabilistic Prediction.

Bayesian probabilistic prediction is typically done based on the posterior predictive distribution

$$\mathbb{P}(Y | X = x) = \int_{\Theta} \mathbb{P}(Y | X = x, \theta) \mathbb{P}(d\theta | D),$$

which plays a central role in Bayesian reasoning and decision-making. The posterior predictive represents our belief about how the outcome variable Y would be distributed were we to observe $X = x$.

There are various ways to make use of this distribution. For instance, when a point prediction is required, the task can be formulated as a decision problem,

$$\hat{y} = \arg \min_{y \in \mathcal{Y}} \mathbb{E}_{\mathbb{P}(Y|X=x)} [\ell(Y, y)],$$

where ℓ denotes a loss function.

To avoid measure-theoretic complications, consider the classification setting and ask the following question: *what is the uncertainty underlying my decision to predict $Y = \hat{y}$?* A simple and intuitive answer is given by

$$1 - \mathbb{P}(Y = \hat{y} \mid X = x),$$

which quantifies how unconfident we are in this particular prediction. **Importantly, this notion of uncertainty is associated with a specific decision — namely, the decision to output the point prediction \hat{y} .**

Beyond point prediction, one may also consider *set-valued predictions*, although this perspective is less commonly emphasised in the machine learning literature. Given a posterior predictive distribution, such predictions can be constructed via the notion of a *highest density region (HDR)*.²

Formally, for a tolerance level $\alpha \in (0, 1)$, the HDR is defined as the smallest region $R_\alpha \subseteq \mathcal{Y}$ satisfying

$$\mathbb{P}(Y \in R_\alpha \mid X = x) = 1 - \alpha.$$

If we now ask

“What is the uncertainty associated with the decision to predict R_α ?”

a natural quantity to consider is

$$1 - \mathbb{P}(Y \in R_\alpha \mid X = x),$$

which equals α by construction. This is entirely expected, since the set-valued prediction itself was explicitly defined through the prescribed tolerance level.

However, if instead we ask

“What uncertainty should be associated with the object produced by the decision to issue a set-valued prediction?”

we are no longer evaluating the uncertainty of the decision, but rather the uncertainty of the resulting object — the region R_α itself. A seemingly natural response is to quantify this uncertainty through the size of the region, measured using an appropriate notion of volume, such as the counting measure in discrete spaces or the Lebesgue measure in continuous ones.

So how does *epistemic predictive uncertainty* enter the picture? As described in the main text, it can be understood as follows:

Epistemic predictive uncertainty refers to the uncertainty arising from reasoning about Y probabilistically in the presence of multiple plausible predictive distributions.

In contrast to decision-based uncertainty — which concerns the reliability of a particular prediction or prediction set — epistemic predictive uncertainty characterises ambiguity at the level of the predictive model itself.

We can summarise these concepts with the following table

²This should not be confused with credible intervals, which characterise uncertainty about model parameters, whereas highest density regions pertain to uncertainty about the outcome variable of interest.

Table 2: Diving deep into what various uncertainties are associated with and how they could be quantified?

Uncertainty associated to	How to measure such uncertainties under Bayesian context
The decision to construct a set-valued prediction at level α	α
The resulting set-valued prediction at level α	set sizes
Reasoning about the outcome variable Y under multiple plausible predictive models	Epistemic predictive uncertainty

A.1.2 Conformal Prediction

Now, what about conformal prediction? To clarify what quantifying epistemic predictive uncertainty truly entails, we draw an analogy with Bayesian prediction.

In the Bayesian framework, the posterior distribution $\mathbb{P}(\theta | D)$ represents uncertainty over a set of plausible models. Analogously, under the consonance assumption, a conformal prediction procedure implicitly induces a credal set of predictive distributions, capturing multiple predictive models consistent with the data and the conformal construction (e.g., the choice of nonconformity score and calibration set).

When making set-valued predictions under model uncertainty, a standard approach is to adopt a worst-case perspective. In particular, given a set of plausible models, one may construct the imprecise highest density region (IHDR; see Definition 3.3). In this case, the uncertainty associated with producing a prediction set at confidence level α is naturally quantified by α itself.

Similarly, once the IHDR—or equivalently, the conformal prediction region (see Proposition 3.4)—is fixed, the uncertainty associated with this set-valued prediction is commonly assessed via its size (e.g., cardinality in classification or length in regression).

Finally, a distinct notion of uncertainty arises when reasoning directly about the outcome variable Y in the presence of multiple plausible predictive models. Unlike the Bayesian setting, where uncertainty is represented by a distribution over models, conformal prediction gives rise to a set of predictive distributions. In this case, epistemic predictive uncertainty is not determined by the size of the prediction set alone, but by the degree of conflicting information among the candidate predictive models.

This perspective closely mirrors the Bayesian treatment of epistemic uncertainty. In Bayesian prediction, mutual information quantifies disagreement—measured in units of predictive entropy—between the posterior predictive distribution and the predictive distribution induced by a fixed parameter, averaged over the posterior parameter distribution. In the credal setting, an analogous role is played by measures that quantify the extent of imprecision within the credal set, for example by evaluating the maximal discrepancy between optimistic and pessimistic expectations over a class of test functions. Conceptually, both approaches aim to measure how strongly plausible predictive models disagree about future outcomes. This perspective, to us, is the biggest novelty we are bringing to the community.

The following table summarises what we discussed.

Table 3: Diving deep into what various uncertainties are associated with and how they could be quantified?

Uncertainty associated to	How to measure such uncertainties under Bayesian context	How to measure such uncertainties under conformal context
The decision to construct a set-valued prediction at level α	α	α
The resulting set-valued prediction at level α	set sizes	set sizes
Reasoning about the outcome variable Y under multiple plausible predictive models	Epistemic predictive uncertainty	Before us, this question was unanswered.

A.2 Is the credal set perspective necessary?

It is natural for readers to wonder about the practical relevance of introducing the full credal set and imprecise probability perspective in this paper, especially given that, in the end, the proposed algorithm for quantifying the EPU of conformal prediction simply reduces to computing the following

Proposition 3.7. *For K -class classification,*

$$\text{MMI}_{\{\pi_x\}}(\overline{\mathbb{P}_x}) = \sum_{k=2}^{K+1} (\pi_{\sigma(k-1)} - \pi_{\sigma(k)}) \cdot \pi_{\sigma(k)},$$

where $\pi_{\sigma(1)} \geq \pi_{\sigma(2)} \cdots \geq \pi_{\sigma(K)}$ are conformal p-values arranged in descending order, and $\pi_{(K+1)} := 0$.

which describes the “shape” of the conformal p-value “distribution”.

At first glance, one might therefore ask whether such a perspective is truly necessary. For instance, a seemingly simpler alternative would be to directly aggregate the conformal p-values—e.g., by summing them—without explicitly appealing to credal sets or imprecise probabilities. However, such an approach would discard the theoretical justification underlying the construction and reduce the method to an intuition-driven heuristic.

More fundamentally, it is not immediately clear how epistemic uncertainty should be quantified solely from this p-value “distribution”. Conformal p-values do not form a probability distribution: they do not sum to one, and interpreting them as probabilities is not theoretically justified. Any attempt to rescale them into a probability distribution and subsequently apply entropy-based measures would therefore be ad hoc, lacking a principled semantic foundation.

In contrast, the credal set perspective provides a coherent interpretative framework in which these p-values arise naturally as lower and upper probabilistic constraints, enabling epistemic uncertainty to be quantified in a principled and well-defined manner.

A.3 How is the epistemic uncertainty discussed here differ from the one in [Sale et al. \(2025\)](#)?

[Sale et al. \(2025\)](#) also discuss aleatoric and epistemic uncertainty within the conformal prediction framework. However, their notion of epistemic uncertainty differs fundamentally from the one considered in this paper. Specifically, they adopt a learning-theoretic perspective, defining epistemic uncertainty as the functional discrepancy between the learned predictor and the ground-truth

prediction function. This viewpoint is primarily motivated by the principle that epistemic uncertainty should diminish as more data are observed.

While conceptually appealing, this definition relies on an unobservable object—the ground-truth prediction function—which is inaccessible in practice. As a result, it does not admit a concrete estimation procedure and therefore remains largely conceptual.

In contrast, our notion of epistemic predictive uncertainty is defined entirely in terms of observable quantities induced by the conformal procedure itself—namely, the difficulty faced by the learner arising from the existence of multiple predictive models that are simultaneously consistent with the data. This definition aligns naturally with information-theoretic treatments of epistemic uncertainty and admits practical estimation procedures that facilitate downstream decision-making.

B Background on Imprecise Probabilities and Imprecise Probabilistic Machine Learning

While conformal prediction is a popular framework that is widely adopted in machine learning, imprecise probabilities and their integration into machine learning, are relatively less known by the broader community. To facilitate readers to better understand our results, we hereby provide some more background information on this topic.

B.1 Imprecise Probabilities

Imprecise probabilities (IP) (Walley, 1991; Troffaes & de Cooman, 2014; Augustin et al., 2014) is a general mathematical framework to deal with uncertainties that cannot be purely captured through a single, precise probability measure alone. This type of uncertainties are often understood as uncertainty arising from ignorance or lack of knowledge, previously termed in various ways, such as ‘Knightian uncertainty’ (Knight, 1921), ‘second-order uncertainty’, or ‘unknown unknowns’. Precise probability struggles to model such types of uncertainty. For instance, it struggles to formally model missing, uncertain, or qualitative data (Cuzzolin, 2020, Section 1.3) and fails to distinguish between indifference (equal belief) and genuine ignorance (absence of knowledge) (Walley, 1991, Section 1.1.4); see also Hájek’s (Hájek, 2019) discussion on Laplace’s and Bertrand’s paradox (Bertrand, 1889). At a more fundamental level, when probability is used to encode subjective belief or confidence, the additivity axiom of Kolmogorov implies that high uncertainty (low confidence) about an event necessarily entails high certainty (high confidence) about its complement. Yet under limited information, this may not hold—we might reasonably remain ambiguous about both.

Mathematically speaking, imprecise probabilities do not admit a single form but comprise a range of methods that attempt to encode higher-order uncertainties in various ways. This includes interval probabilities (Keynes, 1921), random sets (Kingman, 1975), fuzzy measures (Sugeno, 1974), belief functions (Shafer, 1976), higher-order probabilities (Baron, 1987; Gaifman, 1986), possibility theory (Dubois & Prade, 1985), credal sets (Caprio & Gong, 2023; Caprio & Mukherjee, 2023; Caprio & Seidenfeld, 2023; Caprio, 2025a), and lower/upper probabilities (Walley, 1991; Caprio et al., 2024b).

B.2 Imprecise Probabilistic Machine Learning

There has been an uprising momentum of imprecise probabilistic methods adapting to machine learning frameworks, owing to the increasing attention to safety critical applications of ML models, where proper uncertainty management is not only a good-to-have, but critical. This motivation leads to the field of *Imprecise Probabilistic Machine Learning*, which focuses on inference and decision-making using generalisations of classical probability. IPML provides principled tools to handle imprecision arising from model misspecification and data uncertainty, with growing applications in classification (Denoeux, 2000; Zaffalon, 2002; Sale et al., 2023, 2024), hypothesis testing (Chau et al., 2024; Jürgens et al., 2025), scoring rules (Fröhlich & Williamson, 2024; Singh et al., 2025a), conformal prediction (Stutz et al., 2023; Caprio et al., 2025c), computer vision (Cuzzolin & Frezza, 1999; Giunchiglia et al., 2023), probabilistic programming (Liell-Cock & Staton, 2025), explainability (Chau et al., 2023; Utkin et al., 2025; Mohammadi et al., 2026), neural networks (Denoeux, 2000; Caprio et al., 2024a; Wang et al., 2024), learning theory (Caprio et al., 2024c; Sloman et al., 2025), causal inference (Cozman, 2000; Zaffalon et al., 2023), active and continual learning (Dutta et al., 2025; Lu et al., 2025), fixed point theory (Caprio et al., 2025a), and many more.

B.3 Credal Uncertainty Quantification Measures and MMI

Uncertainty modelling generally involves asking the following two questions:

1. How should uncertainty be represented? Should it be a set? a distribution? a set of distributions? Or distribution over sets?
2. After deciding your representation of uncertainty, how can we numerically quantify the degree of uncertainty within such uncertainty representation?

As a simple illustration, one may model the variability of BMI records in a hospital using a probability distribution. Uncertainty can then be quantified in various ways, for example by computing the variance of the distribution or by evaluating its Shannon entropy, which measures the expected “surprise” of outcomes (Stone, 2024).

As discussed in the main text, imprecise probabilistic predictors represent uncertainty about their probabilistic predictions through credal sets $\mathcal{M} \subseteq \mathcal{P}(\mathcal{Y})$. While this specifies the representation of uncertainty—namely, sets of distributions—there remain multiple principled ways to quantify the uncertainty encoded in such credal sets (Hüllermeier & Waegeman, 2021). For example,

1. **Maximal Entropy differences:**

$$\max_{\mathbb{P} \in \mathcal{M}} H(\mathbb{P}) - \min_{\mathbb{Q} \in \mathcal{M}} H(\mathbb{Q})$$

where H is the function that computes the Shannon entropy. This measure is particularly convenient for credal sets represented as the convex hull of a finite collection of distributions, since both extrema can be computed efficiently via standard linear programming. However, in this work, our credal set is generated through the core of the plausibility measure; such tricks cannot be applied here. Also, the entropy difference also suffers from violating the monotonicity properties that usual credal uncertainty measures should satisfy (Abellán et al., 2006), i.e. if $\mathcal{M}_1 \subset \mathcal{M}_2$ then the latter should be quantified larger than the former. With this measure, as long as the smaller credal set \mathcal{M}_1 contains the distributions in the credal set \mathcal{M}_2 corresponding to the maximal and minimal entropies, then their quantified uncertainty is the same.

2. **Generalised Hartley Measure** (Abellán & Klir, 2005), as the name suggests, is a generalisation of the classical Hartley measure (Hartley, 1928) to the imprecise probability setting. For a finite space \mathcal{Y} , and a given lower probability $\underline{\mathbb{P}}$, the generalised Hartley measure can be computed as

$$\sum_{A \subseteq \mathcal{Y}} m_{\underline{\mathbb{P}}}(A) \log_2(|A|)$$

where the mass function $m_{\underline{\mathbb{P}}} : 2^{\mathcal{Y}} \rightarrow [0, 1]$ is the Möbius inverse of $\underline{\mathbb{P}}$, defined as

$$m_{\underline{\mathbb{P}}}(A) = \sum_{B \subseteq A} (-1)^{(|A| - |B|)} \underline{\mathbb{P}}(B).$$

The generalised Hartley measure enjoys several desirable axiomatic properties established in the uncertainty literature (Abellán & Gómez, 2006; Sale et al., 2023). However, its computation is exponential in the outcome space, as it requires summation over all subsets. Moreover, Chau et al. (2025) shows that the generalised Hartley measure and maximum mean imprecision (MMI) yield no empirically distinguishable performance differences in downstream tasks. Since

MMI additionally admits an exact analytical solution computable in linear time, we therefore adopt MMI in this work. Also, a generalised Hartley measure for continuous spaces (e.g. \mathbb{R}) does not exist.

B.3.1 Maximum Mean Imprecision (Chau et al., 2025)

The **Maximum Mean Imprecision** (Chau et al., 2025) is derived based on the idea of an *integral imprecise probability metrics*, defined analogously to the classical integral probability metrics (Müller, 1997). Specifically, denote $C_b(\mathcal{Y})$ as the space of bounded continuous measurable functions from \mathcal{Y} to \mathbb{R} . For a function class $\mathcal{H} \subseteq C_b(\mathcal{Y})$ and two capacities ν, μ (recall Definition 2.1), the integral imprecise probability metric associated with \mathcal{H} between ν and μ is defined as

$$\text{IIPM}_{\mathcal{H}}(\nu, \mu) = \sup_{f \in \mathcal{H}} \left| \int f d\nu - \int f d\mu \right|$$

where $\int f d\nu$ is known as Choquet integral (Choquet, 1953; Troffaes & de Cooman, 2014), and is defined as

$$\int f d\nu = \inf_y f(y) + \int_{\inf_y f(y)}^{\sup_y f(y)} \nu(\{y : f(y) \geq t\}) dt.$$

This defines a valid metric for capacities, provided the test function space is rich enough, e.g., \mathcal{H} is dense in $C_b(\mathcal{Y})$.

The maximum mean imprecision is then simply the result of measuring the discrepancy between an upper probability and its conjugate lower probability through the use of an integral imprecise probability metric. Similarly, given a subset of test functions \mathcal{H} , and an upper probability, the maximum mean imprecision is defined as

$$\text{MMI}_{\mathcal{H}}(\overline{\mathbb{P}_x}) = \sup_{f \in \mathcal{H}} \left| \int f d\overline{\mathbb{P}_x} - \int f d\mathbb{P}_x \right|$$

While Chau et al. (2025) introduced MMI for classification settings only using the total variation distance function class, in this work, we generalise further and consider a specific function class for plausibility measures, which yield computationally efficient analytical forms when computing the MMI for conformal prediction.

C Proofs and derivations

This section presents proofs and derivations in the main text.

C.1 Proof for Proposition 3.2

Proposition 3.2. *Let π_x be consonant, define $\bar{\mathbb{P}}_x$ by*

$$\bar{\mathbb{P}}_x(A) = \sup_{y \in A} \pi_x(y)$$

for all $A \in \mathcal{F}_Y$, with the convention $\bar{\mathbb{P}}_x(\emptyset) := 0$. Then $\bar{\mathbb{P}}_x$ is an upper probability.

Proof. To show $\bar{\mathbb{P}}_x$ is a valid upper probability, we show the following,

1. **Normalisation.** For \emptyset , $\bar{\mathbb{P}}_x(\emptyset) = 0$. For \mathcal{Y} , we have $\bar{\mathbb{P}}_x(\mathcal{Y}) = \sup_{y \in \mathcal{Y}} \pi_x(y) = 1$ due to consonance.
2. **Monotonic.** For $A \subseteq B$ and $A, B \in \mathcal{F}_Y$, it is obvious that $\bar{\mathbb{P}}_x(A) = \sup_{y \in A} \pi_x(y) \leq \sup_{y \in B} \pi_x(y) = \bar{\mathbb{P}}_x(B)$.
3. Consider the core $\mathcal{M}(\bar{\mathbb{P}}_x)$, then it is easy to see that

$$\bar{\mathbb{P}}_x(A) = \sup_{\mathbb{P} \in \mathcal{M}(\bar{\mathbb{P}}_x)} \mathbb{P}(A)$$

for all $A \in \mathcal{F}_Y$. The fact that the core is compact follows from [Marinacci & Montrucchio \(2004, Proposition 3\)](#).

Satisfying points 1 and 2 makes $\bar{\mathbb{P}}_x$ a capacity, satisfying point 3 makes it a valid upper probability. \square

C.2 Proof for Proposition 3.4

Proposition 3.4. *Denote the $(1 - \alpha)$ -IHDR of $\bar{\mathbb{P}}_x$ as $\text{IR}_\alpha^{\mathcal{M}}$. Then, for any $\alpha \in [0, 1]$, we have*

$$\text{IR}_\alpha^{\mathcal{M}} = C_\alpha(x).$$

Proof. The proof follows from [Caprio et al. \(2025c, Proposition 5\)](#). Consider the function $\gamma : \mathcal{Y} \rightarrow [0, 1]$,

$$y \mapsto \gamma(y) = \begin{cases} \pi_x(y), & \text{if } \pi_x(y) \leq 0.5 \\ 1 - \pi_x(y), & \text{if } \pi_x(y) > 0.5. \end{cases} \quad (4)$$

It is easy to see that $\gamma(y) \leq \pi_x(y)$ for all $y \in \mathcal{Y}$. In addition, by the consonance property of π_x , there exists $\tilde{y} \in \mathcal{Y}$ such that $\gamma(\tilde{y}) = 0$. In turn, we have that $[\gamma, \pi]$ forms a cloud ([Augustin et al., 2014, Definition 4.6](#)). Neumaier's probabilistic constraint on clouds ([Augustin et al., 2014, Equation 4.9](#)) gives us

$$\begin{aligned} \mathbb{P}(Y_{n+1} \in C_\alpha) &= \mathbb{P}(Y_{n+1} \in \{y \in \mathcal{Y} : \pi_x(y) > \alpha\}) \\ &\geq 1 - \alpha \\ &= \underline{\mathbb{P}}_x(Y_{n+1} \in \text{IR}_\alpha^{\mathcal{M}}), \end{aligned}$$

for all $\mathbb{P} \in \mathcal{M}(\overline{\mathbb{P}}_x)$ and $\underline{\mathbb{P}}_x$ is the lower probability with respect to $\overline{\mathbb{P}}_x$. In turn, we have

$$\begin{aligned}\underline{\mathbb{P}}_x(Y_{n+1} \in C_\alpha(x)) &= \underline{\mathbb{P}}_x(Y_{n+1} \in \{y \in \mathcal{Y} : \pi_x(y) > \alpha\}) \\ &\geq 1 - \alpha \\ &= \underline{\mathbb{P}}_x(Y_{n+1} \in \text{IR}_\alpha^{\mathcal{M}}).\end{aligned}$$

Since the imprecise highest density region $\text{IR}_\alpha^{\mathcal{M}}$ is the smallest subset that attains lower probability $1 - \alpha$, it implies that $\text{IR}_\alpha^{\mathcal{M}} \subseteq C_\alpha(x)$. However, by the definition of CPR, $\text{IR}_\alpha^{\mathcal{M}}$ cannot be strictly included in $C_\alpha(x)$. In turn, this implies that $\text{IR}_\alpha^{\mathcal{M}} = C_\alpha(x)$. \square

C.3 Proof for Proposition 3.5

Proposition 3.5. *Let $\mathcal{H}_{TV} = \{\mathbf{1}_A : A \in \mathcal{F}_{\mathcal{Y}}\}$. Then*

$$\text{MMI}_{\mathcal{H}_{TV}}(\overline{\mathbb{P}}_x) = \sup_{A \in \mathcal{F}_{\mathcal{Y}}} |\overline{\mathbb{P}}_x(A) - \underline{\mathbb{P}}_x(A)| = \pi_{\sigma(2)},$$

where $\pi_{\sigma(2)}$ denotes the second largest conformal p-value.

Proof. Under consonance, there exists \tilde{y} such that $\pi_x(\tilde{y}) = 1$. Now, recall the definition of MMI,

$$\begin{aligned}\text{MMI}_{\mathcal{H}_{TV}}(\overline{\mathbb{P}}_x) &= \sup_{A \in \mathcal{F}_{\mathcal{Y}}} |\overline{\mathbb{P}}_x(A) - \underline{\mathbb{P}}_x(A)| \\ &= \sup_{A \in \mathcal{F}_{\mathcal{Y}}} |\overline{\mathbb{P}}_x(A) - (1 - \overline{\mathbb{P}}_x(A^c))| \\ &= \sup_{A \in \mathcal{F}_{\mathcal{Y}}} |\overline{\mathbb{P}}_x(A) + \overline{\mathbb{P}}_x(A^c) - 1| \\ &= |\overline{\mathbb{P}}_x(\{\tilde{y}\}) - 1 + \overline{\mathbb{P}}_x(\{\tilde{y}\}^c)| \\ &= |\overline{\mathbb{P}}_x(\{\tilde{y}\}^c)| \\ &= \pi_{\sigma(2)}\end{aligned}$$

The key observation is that the quantity $|\overline{\mathbb{P}}_x(A) + \overline{\mathbb{P}}_x(A^c) - 1|$ is maximised when $A = \{\tilde{y}\}$. By consonance, this singleton contains the label with the largest conformal p-value, which is equal to 1. Consequently, $\overline{\mathbb{P}}_x(A) = 1$, while $\overline{\mathbb{P}}_x(A^c)$ attains the second-largest conformal p-value $\pi_{\sigma(2)}$. \square

C.4 Proof for Proposition 3.6

Proposition 3.6. *Let π_x be consonant and $\overline{\mathbb{P}}_x$ the induced plausibility measure. Then,*

$$\text{MMI}_{\{\pi_x\}}(\overline{\mathbb{P}}_x) = \int_0^1 \sup_{y \notin C_\alpha(x)} \pi_x(y) d\alpha \tag{2}$$

$$= \int_0^1 (1 + n_{cal})^{-1} (1 + |B_\alpha|) d\alpha, \tag{3}$$

where $B_\alpha = \{S_i \in S_{cal} : S_i \geq \inf_{y \notin C_\alpha(x)} s(x, y)\}$.

Proof. Under consonance, there exists \tilde{y} such that $\pi_x(\tilde{y}) = 1$. Now, expanding MMI, we have

$$\begin{aligned}
\text{MMI}_{\{\pi_x\}}(\overline{\mathbb{P}_x}) &= \oint \pi_x d\overline{\mathbb{P}_x} - \oint \pi_x d\underline{\mathbb{P}_x} \\
&= \int_0^1 \overline{\mathbb{P}_x}(\{y \in \mathcal{Y} : \pi_x(y) \geq \alpha\}) d\alpha - \int_0^1 \underline{\mathbb{P}_x}(\{y \in \mathcal{Y} : \pi_x(y) \geq \alpha\}) d\alpha \\
&= \int_0^1 \sup_{y \in C_\alpha(x)} \pi_x(y) d\alpha - \left(1 - \int_0^1 \overline{\mathbb{P}_x}(\{y \in \mathcal{Y} : \pi_x(y) < \alpha\}) d\alpha\right) \\
&= 1 - 1 + \int_0^1 \overline{\mathbb{P}_x}(\{y \in \mathcal{Y} : \pi_x(y) < \alpha\}) d\alpha \\
&= \int_0^1 \sup_{y \notin C_\alpha(x)} \pi_x(y) d\alpha \\
&= \int_0^1 \sup_{y \notin C_\alpha(x)} \frac{1 + |\{S_i \in S_{\text{cal}} : S_i \geq s(x, y)\}|}{1 + n_{\text{cal}}} d\alpha \\
&= \int_0^1 \frac{1 + |\{S_i \in S_{\text{cal}} : S_i \geq \inf_{y \notin C_\alpha(x)} s(x, y)\}|}{1 + n_{\text{cal}}} d\alpha \\
&= \int_0^1 \frac{1 + |B_\alpha|}{1 + n_{\text{cal}}} d\alpha.
\end{aligned}$$

The key observation for this proof is that due to consonance, the integral $\int_0^1 \max_{y \in C_\alpha(x)} \pi_x(y) d\alpha = \int_0^1 1 d\alpha$, therefore it becomes 1. \square

C.5 Proof for Proposition 3.7

Proposition 3.7. *For K-class classification,*

$$\text{MMI}_{\{\pi_x\}}(\overline{\mathbb{P}_x}) = \sum_{k=2}^{K+1} (\pi_{\sigma(k-1)} - \pi_{\sigma(k)}) \cdot \pi_{\sigma(k)},$$

where $\pi_{\sigma(1)} \geq \pi_{\sigma(2)} \geq \dots \geq \pi_{\sigma(K)}$ are conformal p-values arranged in descending order, and $\pi_{(K+1)} := 0$.

Proof. Utilising results proven from Proposition 3.6, we start from

$$\begin{aligned}
\text{MMI}_{\{\pi_x\}}(\overline{\mathbb{P}_x}) &= \int_0^1 \sup_{y \notin C_\alpha(x)} \pi_x(y) d\alpha \\
&= \int_0^1 \sum_{k=2}^{K+1} \sup_{y \notin C_\alpha(x)} \pi_x(y) \mathbf{1} \left[\sup_{y \notin C_\alpha(x)} \pi_x(y) = \pi_{\sigma(k)} \right] d\alpha \\
&= \sum_{k=2}^{K+1} \pi_{\sigma(k)} \int_0^1 \mathbf{1} \left[\sup_{y \notin C_\alpha(x)} \pi_x(y) = \pi_{\sigma(k)} \right] d\alpha \\
&\stackrel{\diamond}{=} \sum_{k=2}^{K+1} (\pi_{\sigma(k-1)} - \pi_{\sigma(k)}) \cdot \pi_{\sigma(k)}.
\end{aligned}$$

To see why step \diamond holds, consider “sweeping” α upwards from 0, then there are $\pi_{\sigma(K)}$ amount of “time” that the set

$$C_\alpha(x)^c = \{y \in \mathcal{Y} : \pi_x(y) < \alpha\}$$

is empty. As we keep increasing α , the first time this set $C_\alpha(x)^c$ becomes non-empty is when α is sandwiched between $\pi_{\sigma(K-1)}$ and $\pi_{\sigma(K)}$, which then

$$\overline{\mathbb{P}_x}(C_\alpha(x)^c) = \pi_{\sigma(K)}.$$

Now keep increasing α , keeping track of how much “time” α stays when $\overline{\mathbb{P}_x}(C_\alpha(x)^c) = \pi_{\sigma(k)}$. Now, sum up these fragments, and you get the full sum.

□

C.6 Proof for Proposition 3.8

Proposition 3.8. *In conformal regression, for score functions satisfying $\inf_{y \notin C_\alpha(x)} s(x, y) = \hat{q}_{1-\alpha}$,*

$$\text{MMI}_{\{\pi_x\}}(\overline{\mathbb{P}_x}) = 1 + \int_0^1 \frac{1 - \lceil (n_{\text{cal}} + 1)(1 - \alpha) \rceil}{n_{\text{cal}} + 1} d\alpha.$$

Proof. Starting with the expression

$$\begin{aligned} \text{MMI}_{\{\pi_x\}}(\overline{\mathbb{P}_x}) &= \int_0^1 \sup_{y \notin C_\alpha(x)} \pi_x(y) d\alpha \\ &= \int_0^1 \sup_{y \notin C_\alpha(x)} \frac{1 + |\{S_i \in S_{\text{cal}} : S_i \geq s(x, y)\}|}{1 + n_{\text{cal}}} d\alpha \\ &= \int_0^1 \frac{1 + |\{S_i \in S_{\text{cal}} : S_i \geq \inf_{y \notin C_\alpha(x)} s(x, y)\}|}{1 + n_{\text{cal}}} d\alpha \\ &= \int_0^1 \frac{1 + |B_\alpha|}{1 + n_{\text{cal}}} d\alpha. \end{aligned}$$

Now, if there exists $y \notin C_\alpha(x)$ such that $s(x, y) = \hat{q}_{1-\alpha}$, then by the definition of empirical $(1 - \alpha)$ quantile, we have

$$\begin{aligned} |B_\alpha| &= |\{S_i : S_i \geq \hat{q}_{1-\alpha}\}| \\ &= n_{\text{cal}} + 1 - \lceil (n_{\text{cal}} + 1)(1 - \alpha) \rceil \end{aligned}$$

therefore,

$$\text{MMI}_{\{\pi_x\}}(\overline{\mathbb{P}_x}) = 1 + \int_0^1 \frac{1 - \lceil (n_{\text{cal}} + 1)(1 - \alpha) \rceil}{n_{\text{cal}} + 1} d\alpha. \quad (5)$$

The key observation is to realise that the supremum of the fraction is realised when $y \notin C_\alpha(x)$ is chosen such that $s(x, y)$ is as small as possible. Now for the score functions we consider,

- For **Absolute residual error** $s_1(x, y) = |\hat{f}(x) - y|$, we know $\inf_{y \notin C_\alpha(x)} s_1(x, y)$ is attained when $y^* = \hat{f}(x) + \hat{q}_{1-\alpha}$, in that case, we have

$$\begin{aligned} \inf_{y \notin C_\alpha(x)} s_1(x, y) &= s_1(x, y^*) \\ &= |\hat{f}(x) - \hat{f}(x) - \hat{q}_{1-\alpha}| \\ &= \hat{q}_{1-\alpha} \end{aligned}$$

therefore, by the definition of empirical $(1 - \alpha)$ quantile, we have

$$\begin{aligned} |B_\alpha| &= |\{S_i : S_i \geq \hat{q}_{1-\alpha}\}| \\ &= (n_{\text{cal}} + 1) - \lceil (n_{\text{cal}} + 1)(1 - \alpha) \rceil \end{aligned}$$

- Similarly, for **Weighted residual error** $s_2(x, y) = \frac{|y - \hat{f}(x)|}{w(x)}$, we know the infimum $\inf_{y \notin C_\alpha} s_2(x, y)$ is attained when $y^* = \hat{f}(x) + w(x)\hat{q}_{1-\alpha}$. In that case, again, we have

$$\begin{aligned}\inf_{y \notin C_\alpha(x)} s_2(x, y) &= s_2(x, y^*) \\ &= |\hat{f}(x) - \hat{f}(x) - w(x)\hat{q}_{1-\alpha}|/w(x) \\ &= \hat{q}_{1-\alpha}.\end{aligned}$$

With the same reasoning as above, $|B_\alpha| = (n_{\text{cal}} + 1) - \lceil (n_{\text{cal}} + 1)(1 - \alpha) \rceil$.

- For **quantile regression scores** $s_3(x, y) = \max(\hat{f}_\ell(x) - y, y - \hat{f}_u(x))$, the infimum is attained when y takes the value $\hat{f}_u(x) + \hat{q}_{1-\alpha}$, which similarly then result in

$$\inf_{y \notin C_\alpha(x)} s_3(x, y) = \hat{q}_{1-\alpha},$$

which leads to $|B_\alpha| = (n_{\text{cal}} + 1) - \lceil (n_{\text{cal}} + 1)(1 - \alpha) \rceil$.

Therefore, regardless of choosing s_1, s_2, s_3 , as long as $\inf_{y \notin C_\alpha(x)} s(x, y) = \hat{q}_{1-\alpha}$, we get

$$\text{MMI}_{\{\pi_x\}}(\overline{\mathbb{P}_x}) = 1 + \int_0^1 \frac{1 - \lceil (n_{\text{cal}} + 1)(1 - \alpha) \rceil}{1 + n_{\text{cal}}} d\alpha.$$

□

C.7 Proof for Proposition 3.9

Proposition 3.9. Let $\tilde{\pi}_x$ be the modified consonant transducer from the original transducer π_x . Let $\tilde{C}_\alpha(\cdot)$ be the CPR constructed using $\tilde{\pi}_x$. Then, for any test instances x , it is true that

1. we have

$$\tilde{C}_\alpha(x) \setminus C_\alpha(x) = \{y_{\sigma(1)}\}$$

if and only if $C_\alpha(x) = \emptyset$, otherwise

$$\tilde{C}_\alpha(x) = C_\alpha(x).$$

2. For prediction on unseen data (X_{n+1}, Y_{n+1}) , the marginal coverage guarantee is preserved, i.e.

$$\mathbb{P}(Y_{n+1} \in \tilde{C}_\alpha(X_{n+1})) \geq 1 - \alpha.$$

Proof. Let $\tilde{\pi}_x$ be the modified consonant transducer from the original conformal transducer π , following the construction outlined in Equation 1.

Point 1: To show the first point, consider the two complementary scenario

1. When α is chosen such that for all labels $y \in \mathcal{Y}$, $\pi_x(y) < \alpha$, then $C_\alpha(x) = \emptyset$. In this case, since the label with the largest conformal p-value is now assigned 1, the set $\tilde{C}_\alpha(x)$ will instead return $\{y_{\sigma(1)}\}$ as the prediction set.
2. When α is chosen such that there exists at least one label $y \in \mathcal{Y}$, such that $\pi_x(y) > \alpha$, then the label with the largest conformal p-value must be within the set $\{y : \pi_x(y) > \alpha\}$, as such, even if we stretch the conformal p-value to 1, it does not affect the prediction set at all, since that label already belongs to the prediction set.

Point 2: To show the second point, recall that no matter which α we choose, we always have

$$C_\alpha(x) \subseteq \tilde{C}_\alpha(x).$$

Therefore, since for any data (X_{n+1}, Y_{n+1}) , we have the conformal guarantee of

$$\mathbb{P}(Y_{n+1} \in C_\alpha(X_{n+1})) \geq 1 - \alpha,$$

then we have,

$$\begin{aligned} \mathbb{P}(Y_{n+1} \in \tilde{C}_\alpha(X_{n+1})) &\geq \mathbb{P}(Y_{n+1} \in C_\alpha(X_{n+1})) \\ &\geq 1 - \alpha, \end{aligned}$$

therefore also satisfying the usual marginal guarantee. \square

C.8 Proof for Theorem 3.10

Theorem 3.10 (Uniform validity of consonance conformal prediction (Cella & Martin, 2022)). *Consonance conformal transducers yield a conformal procedure that is uniformly valid, that is*

$$\mathbb{P}(\pi_{X_{n+1}}(Y_{n+1}) \leq \alpha) \leq \alpha,$$

for all n and exchangeable \mathbb{P} . Moreover, uniform validity is equivalent to satisfying

$$\mathbb{P}\left(\left\{\overline{\mathbb{P}_{X_{n+1}}}(A) \leq \alpha \text{ and } Y_{n+1} \in A \text{ for some } A\right\}\right) \leq \alpha$$

for all n, α and exchangeable \mathbb{P} .

Proof. The result is immediate from Cella & Martin (2022, Theorem 1). \square

D Experimental details and further ablation studies

Experimental setup. We provide experimental details in this appendix. All experiments were conducted on a MacBook Pro equipped with an Apple M4 Pro chip, a part of our code is built on the Python module TorchCP (Huang et al., 2024).

In both the active learning and selective classification experiments, we assume access to a single predictive model $\hat{f} : \mathcal{X} \rightarrow \Delta_{K-1}$. We quantify the difficulty of predicting $f(X_{n+1})$ using the various epistemic predictive uncertainty (EPU) measures proposed in this work, such MMI-based ones and the set sizes measured at different level of α .

Overall, both experimental settings rely on the mapping

$$X_{n+1} \mapsto (\hat{f}(X_{n+1}), \text{EPU}(X_{n+1})),$$

where $\text{EPU}(X_{n+1})$ denotes the quantified epistemic uncertainty at X_{n+1} . Depending on the method, this may correspond either to prediction-set sizes or to our proposed MMI-based measures.

Predictions are made solely based on $\hat{f}(X_{n+1})$, while downstream decisions—such as selecting the next point to query in active learning or deciding whether to abstain in selective classification—are driven by $\text{EPU}(X_{n+1})$.

Active learning. In active learning, we used the following four datasets,

1. **Digits v1:** This digit dataset is used in Jain et al. (2000) and is one of a set of 6 datasets describing features of handwritten numerals (0 - 9) extracted from a collection of Dutch utility maps. Corresponding patterns in different datasets correspond to the same original character. 200 instances per class (for a total of 2000 instances) have been digitised in binary images. It has 10 classes with 216 features.
2. **Digits v2:** This dataset corresponds to the *Optical Recognition of Handwritten Digits* (optdigits) (Alpaydin & Kaynak, 1998) dataset from the OpenML repository. It contains 5,620 instances across 10 classes, with 64 input features.
3. **Digits v3:** This digit dataset is also based on the ones used in Jain et al. (2000) and is also one of a set of 6 datasets describing features of handwritten numerals (0 - 9) extracted from a collection of Dutch utility maps. The attributes represent 64 descriptors from the Karhunen-Loeve Transform, a linear transform that corresponds to the projection of the images on the eigenvectors of a covariance matrix.
4. **Letters:** We use the Letter Image Recognition dataset introduced by Frey & Slate (1991). The task is to classify black-and-white rectangular pixel displays into one of the 26 uppercase letters of the English alphabet. The dataset is constructed from 20 different fonts, where each letter instance is randomly distorted to generate a total of 20,000 unique stimuli. Each stimulus is represented by 16 numerical attributes, including statistical moments and edge-count features, which are scaled to integer values in the range [0, 15].

For each dataset, we train a random forest classifier with 100 trees, using randomly initialised models and 100, 100, 100, and 500 training observations for the four datasets, respectively. Prediction is tested against our withheld test dataset that is of 20% size of the whole dataset.

Selective Classification. For selective classification, we evaluate our methods on standard benchmark datasets, including CIFAR10 and CIFAR100 (Krizhevsky & Hinton, 2009), CALTECH101 (Fei-Fei et al., 2004), and FashionMNIST (Xiao et al., 2017). For CIFAR10, we employ pretrained ResNet56 model weights provided by PyTorch (Paszke et al., 2019) as the base predictive model. For CIFAR100, we use pretrained ResNet20 weights. For CALTECH101 and FashionMNIST, we adopt ResNet18 and ResNet34 architectures, respectively, with pretrained weights obtained from HuggingFace.

D.1 Statistical Significance tables

We report here the statistical significance results for the experiments presented in the main text. For both the active learning and selective classification settings, we compare model performance across random seeds—specifically, the final-stage accuracy for active learning and the area under the curve (AUC) for selective classification. Since the same data splits and random seeds are shared across methods, these comparisons yield paired observations. Accordingly, a standard and widely adopted approach is to apply the Wilcoxon signed-rank test to assess whether the observed performance differences are statistically significant. Specifically, the null is that the methods perform similarly, against the alternative that a particular method performs better than the other in terms of the metric. For computing the test error we randomly pick 1000 samples from the test data loader in these modules.

Table 4: (Digits v1 dataset) Statistical significance table for **active learning**. Entries in cell i, j reports the p-value for the one-sided Wilcoxon signed rank test. p-value less than 0.05 (highlighted in red) implies method i is better than method j significantly.

	$ C_{0.01}(\cdot) $	$ C_{0.05}(\cdot) $	$ C_{0.1}(\cdot) $	$ C_{0.2}(\cdot) $	$ C_{0.3}(\cdot) $	MMI-CP(sum)	MMI-CP(sup)
$ C_{0.01}(\cdot) $	NaN	1.000	0.997	1.000	1.000	1.000	1.000
$ C_{0.05}(\cdot) $	0.001	NaN	0.068	0.476	0.500	0.982	0.169
$ C_{0.1}(\cdot) $	0.007	0.932	NaN	0.920	0.902	0.997	0.784
$ C_{0.2}(\cdot) $	0.001	0.524	0.116	NaN	0.500	0.994	0.209
$ C_{0.3}(\cdot) $	0.001	0.539	0.098	0.500	NaN	0.966	0.278
MMI-CP(sum)	0.001	0.018	0.005	0.006	0.034	NaN	0.010
MMI-CP(sup)	0.001	0.831	0.246	0.791	0.784	0.990	NaN

Table 5: (Digits v2 dataset) Statistical significance table for **active learning**. Entries in cell i, j reports the p-value for the one-sided Wilcoxon signed rank test. p-value less than 0.05 (highlighted in red) implies method i is better than method j significantly.

	$ C_{0.01}(\cdot) $	$ C_{0.05}(\cdot) $	$ C_{0.1}(\cdot) $	$ C_{0.2}(\cdot) $	$ C_{0.3}(\cdot) $	MMI-CP(sum)	MMI-CP(sup)
$ C_{0.01}(\cdot) $	NaN	1.000	1.000	1.000	1.000	1.000	1.000
$ C_{0.05}(\cdot) $	0.001	NaN	0.461	0.781	0.800	0.998	1.000
$ C_{0.1}(\cdot) $	0.001	0.615	NaN	0.754	0.935	1.000	0.999
$ C_{0.2}(\cdot) $	0.001	0.219	0.278	NaN	0.694	0.998	1.000
$ C_{0.3}(\cdot) $	0.001	0.200	0.080	0.306	NaN	1.000	1.000
MMI-CP(sum)	0.001	0.003	0.001	0.003	0.001	NaN	0.257
MMI-CP(sup)	0.001	0.001	0.002	0.001	0.001	0.743	NaN

Table 6: (Digits v3 dataset) Statistical significance table for **active learning**. Entries in cell i, j reports the p-value for the one-sided Wilcoxon signed rank test. p-value less than 0.05 (highlighted in red) implies method i is better than method j significantly.

	$ C_{0.01}(\cdot) $	$ C_{0.05}(\cdot) $	$ C_{0.1}(\cdot) $	$ C_{0.2}(\cdot) $	$ C_{0.3}(\cdot) $	MMI-CP(sum)	MMI-CP(sup)
$ C_{0.01}(\cdot) $	NaN	0.992	0.997	1.000	1.000	1.000	1.000
$ C_{0.05}(\cdot) $	0.008	NaN	0.813	1.000	0.997	0.990	0.920
$ C_{0.1}(\cdot) $	0.005	0.216	NaN	0.903	0.813	0.968	0.663
$ C_{0.2}(\cdot) $	0.001	0.001	0.116	NaN	0.240	0.584	0.035
$ C_{0.3}(\cdot) $	0.001	0.007	0.216	0.760	NaN	0.754	0.162
MMI-CP(sum)	0.001	0.014	0.032	0.416	0.313	NaN	0.053
MMI-CP(sup)	0.001	0.116	0.337	0.965	0.838	0.947	NaN

Table 7: (Letters dataset) Statistical significance table for **active learning**. Entries in cell i, j reports the p-value for the one-sided Wilcoxon signed rank test. p-value less than 0.05 (highlighted in red) implies method i is better than method j significantly.

	$ C_{0.01}(\cdot) $	$ C_{0.05}(\cdot) $	$ C_{0.1}(\cdot) $	$ C_{0.2}(\cdot) $	$ C_{0.3}(\cdot) $	MMI-CP(sum)	MMI-CP(sup)
$ C_{0.01}(\cdot) $	NaN	0.991	0.999	1.000	1.000	1.000	1.000
$ C_{0.05}(\cdot) $	0.009	NaN	0.968	0.994	0.976	0.988	0.976
$ C_{0.1}(\cdot) $	0.002	0.042	NaN	0.500	0.348	0.690	0.405
$ C_{0.2}(\cdot) $	0.001	0.006	0.539	NaN	0.237	0.696	0.428
$ C_{0.3}(\cdot) $	0.001	0.042	0.688	0.763	NaN	0.813	0.583
MMI-CP(sum)	0.001	0.012	0.310	0.304	0.216	NaN	0.275
MMI-CP(sup)	0.001	0.042	0.595	0.572	0.417	0.725	NaN

Table 8: (FMNIST dataset) Statistical significance table for **selective classification experiments**. Entries in cell i, j report the p-value for the one-sided Wilcoxon signed rank test. p-value less than 0.05 (highlighted in red) implies method i is better than method j significantly.

	$ C_{0.01}(\cdot) $	$ C_{0.05}(\cdot) $	$ C_{0.1}(\cdot) $	$ C_{0.2}(\cdot) $	$ C_{0.3}(\cdot) $	MMI-CP(sum)	MMI-CP(sup)
$ C_{0.01}(\cdot) $	NaN	0.005	0.003	0.014	0.014	0.065	0.571
$ C_{0.05}(\cdot) $	0.997	NaN	0.577	0.882	0.947	0.958	1.000
$ C_{0.1}(\cdot) $	0.998	0.461	NaN	0.539	0.839	0.884	0.997
$ C_{0.2}(\cdot) $	0.990	0.118	0.500	NaN	0.652	0.779	1.000
$ C_{0.3}(\cdot) $	0.993	0.065	0.188	0.385	NaN	0.839	0.999
MMI-CP(sum)	0.947	0.042	0.138	0.221	0.216	NaN	0.997
MMI-CP(sup)	0.429	0.001	0.007	0.001	0.002	0.005	NaN

Table 9: (CIFAR10 dataset) Statistical significance table for **selective classification experiments**. Entries in cell i, j report the p-value for the one-sided Wilcoxon signed rank test. p-value less than 0.05 (highlighted in red) implies method i is better than method j significantly.

	$ C_{0.01}(\cdot) $	$ C_{0.05}(\cdot) $	$ C_{0.1}(\cdot) $	$ C_{0.2}(\cdot) $	$ C_{0.3}(\cdot) $	MMI-CP(sum)	MMI-CP(sup)
$ C_{0.01}(\cdot) $	NaN	0.001	0.001	0.001	0.001	0.993	0.920
$ C_{0.05}(\cdot) $	1.000	NaN	0.010	0.001	0.001	1.000	0.999
$ C_{0.1}(\cdot) $	1.000	0.993	NaN	0.003	0.005	1.000	0.999
$ C_{0.2}(\cdot) $	1.000	1.000	0.998	NaN	0.097	1.000	0.999
$ C_{0.3}(\cdot) $	1.000	1.000	0.997	0.920	NaN	1.000	1.000
MMI-CP(sum)	0.010	0.001	0.001	0.001	0.001	NaN	0.615
MMI-CP(sup)	0.097	0.002	0.002	0.002	0.001	0.423	NaN

Table 10: (CALTECH101 dataset) Statistical significance table for **selective classification experiments**. Entries in cell i, j report the p-value for the one-sided Wilcoxon signed rank test. p-value less than 0.05 (highlighted in red) implies method i is better than method j significantly.

	$ C_{0.01}(\cdot) $	$ C_{0.05}(\cdot) $	$ C_{0.1}(\cdot) $	$ C_{0.2}(\cdot) $	$ C_{0.3}(\cdot) $	MMI-CP(sum)	MMI-CP(sup)
$ C_{0.01}(\cdot) $	NaN	0.385	0.019	0.001	0.001	0.999	1.000
$ C_{0.05}(\cdot) $	0.652	NaN	0.002	0.001	0.001	1.000	1.000
$ C_{0.1}(\cdot) $	0.986	0.999	NaN	0.001	0.001	1.000	1.000
$ C_{0.2}(\cdot) $	1.000	1.000	1.000	NaN	0.065	1.000	1.000
$ C_{0.3}(\cdot) $	1.000	1.000	1.000	0.947	NaN	1.000	1.000
MMI-CP(sum)	0.002	0.001	0.001	0.001	0.001	NaN	0.385
MMI-CP(sup)	0.001	0.001	0.001	0.001	0.001	0.652	NaN

Table 11: (CIFAR100 dataset) Statistical significance table for **selective classification experiments**. Entries in cell i, j report the p-value for the one-sided Wilcoxon signed rank test. p-value less than 0.05 (highlighted in red) implies method i is better than method j significantly.

	$ C_{0.01}(\cdot) $	$ C_{0.05}(\cdot) $	$ C_{0.1}(\cdot) $	$ C_{0.2}(\cdot) $	$ C_{0.3}(\cdot) $	MMI-CP(sum)	MMI-CP(sup)
$ C_{0.01}(\cdot) $	NaN	1.000	0.976	0.001	0.001	1.000	1.000
$ C_{0.05}(\cdot) $	0.001	NaN	0.014	0.001	0.001	1.000	1.000
$ C_{0.1}(\cdot) $	0.032	0.990	NaN	0.001	0.001	1.000	1.000
$ C_{0.2}(\cdot) $	1.000	1.000	1.000	NaN	0.005	1.000	1.000
$ C_{0.3}(\cdot) $	1.000	1.000	1.000	0.997	NaN	1.000	1.000
MMI-CP(sum)	0.001	0.001	0.001	0.001	0.001	NaN	0.080
MMI-CP(sup)	0.001	0.001	0.001	0.001	0.001	0.935	NaN

Active learning results

D.2 Ablation study on the choice of nonconformity scores

In this ablation study, we investigate how the choice of nonconformity score influences the empirical results. Our theoretical analysis is largely score-agnostic, with the exception of Proposition 3.8,

which specifically concerns conformal regression. To examine the practical impact of different score functions, we consider the following alternatives:

1. LAC: Least Ambiguous Classifiers (LAC)
2. APS: Adaptive Prediction Sets (APS) (Romano et al., 2020), the score we considered in the main text.
3. RAPS: Regularised Adaptive Prediction Sets (Angelopoulos et al., 2021)
4. Margins: Margin non-conformity score (Löfström et al., 2015)
5. EntmaxScore: Score functions based on gamma-entmax transformations (Campos et al., 2025)

We then rerun the selective classification experiments on the CIFAR-100 dataset using each score; the experimental configurations are entirely identical to the ones run in the main text, only the score is different. The results are shown in Figure 6. Overall, we observe that both MMI-based approaches consistently outperform methods based solely on prediction set size, indicating that their empirical advantage is robust to the choice of nonconformity score. This behaviour is intuitive: although different nonconformity scores affect how conformal prediction constructs conformal p-values, both MMI and prediction set size ultimately rely on the same information encoded by these p-values. The observed performance gap, therefore, again suggests that MMI is able to extract richer information about the underlying epistemic uncertainty induced by conformal prediction, beyond what is captured by set size alone.

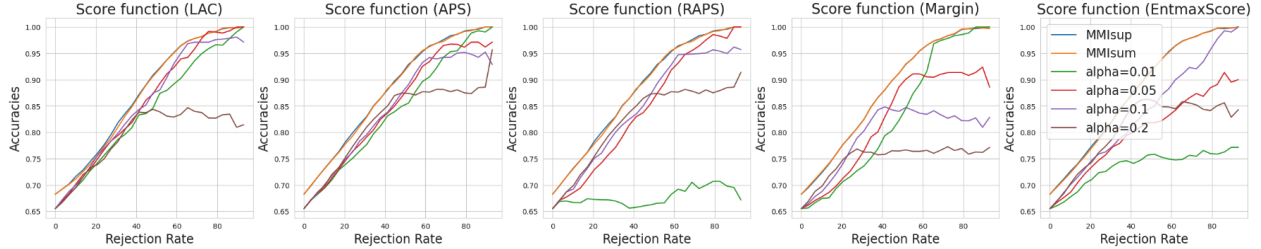


Figure 6: Examining how the choice of nonconformity score affects performance in selective classification on the CIFAR-100 dataset.

D.3 Ablation study on the sizes of the calibration set

Unlike full conformal prediction, split conformal prediction introduces an additional algorithmic component that can influence the resulting CP procedure: the choice of the calibration set. Here we ask ourselves, how does the calibration set size, when keeping every other experimental condition the same, affect the ranking of the methods? We fix the experimental conditions for the selective classification experiments using the CIFAR100 dataset. The results are shown in Figure 7. We see that the overall ranking of various approaches stays consistent, and MMI-based methods still outperform the rest.

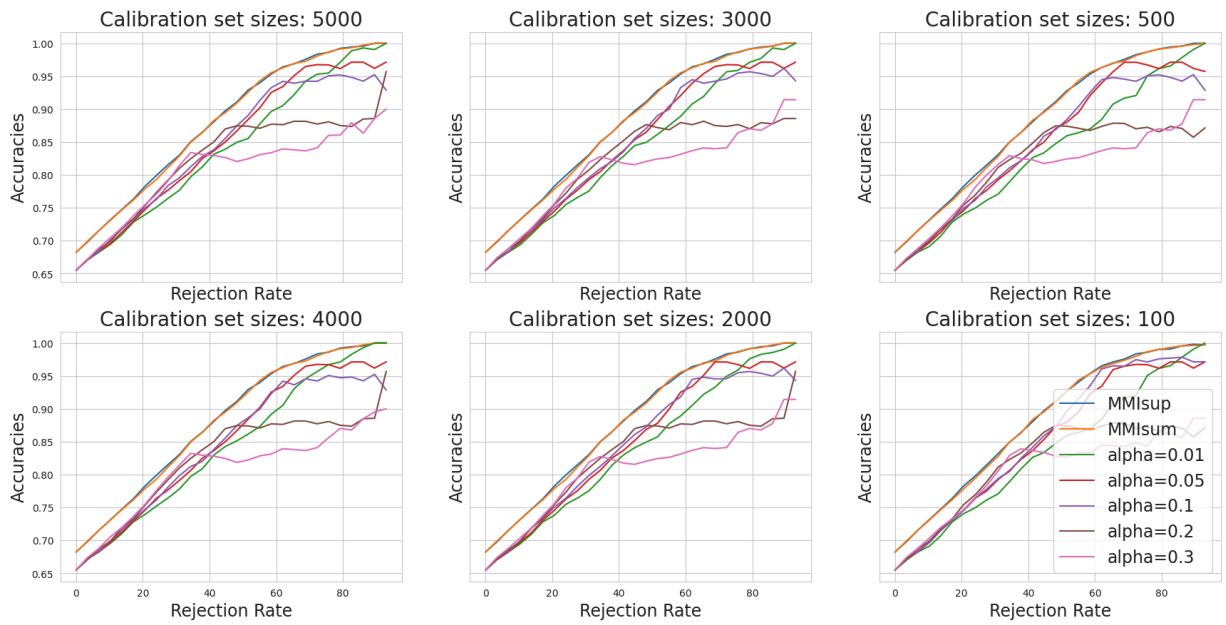


Figure 7: Selective classification results as we vary the number of calibration set sizes. The overall ranking of various approaches stays consistent. MMI-based methods still outperform the rest.